Space WastE Examining Project (SWEEP) Critical Design Review

Corey Crossen*, Demokritos Frangos†, Dillon Briggs ‡, Nicholas Lehnertz §, Raul Rosas ¶, Spencer Little ‖,Stephen Hall **
Arizona State University, Tempe, Arizona, 85287

Space debris in Low Earth Obit is becoming an increasingly large risk to current and future spacecraft. Current ground based systems can only detect 10 mm or larger debris and yet a 1mm object traveling at 10 km/s can seriously damage a spacecraft. This paper proposes a technical demonstration of how a space based vehicle can be capable of detecting and mapping debris 1mm and larger to mitigate the risk of future in flight collisions.

*Student, School for Engineering of Matter, Transport & Energy, 501 E Tyler Mall, Tempe, AZ 85287
†Student, School for Engineering of Matter, Transport & Energy, 501 E Tyler Mall, Tempe, AZ 85287
‡Student, School for Engineering of Matter, Transport & Energy, 501 E Tyler Mall, Tempe, AZ 85287
§Student, School for Engineering of Matter, Transport & Energy, 501 E Tyler Mall, Tempe, AZ 85287
¶Student, School for Engineering of Matter, Transport & Energy, 501 E Tyler Mall, Tempe, AZ 85287
‖Student, School for Engineering of Matter, Transport & Energy, 501 E Tyler Mall, Tempe, AZ 85287
**Student, School for Engineering of Matter, Transport & Energy, 501 E Tyler Mall, Tempe, AZ 85287

Table of Contents

Nomenclature

A	=	Camera Aperature Size
a	=	SemiMajor Axis
b	=	SemiMinor Axis
c	=	Speed of Light
e	=	Eccentricity
γ	=	Angle from Center line
h	=	Planck Constant
HFC	=	Height from Center Line
hn	=	Corresponding Pixel Height
i	=	Inclination
L	=	Size of detectable debris
λ	=	Laser Wavelength
m	=	Mass
N	=	Number of Photons
ω	=	Argument of Periapsis
P	=	Power
R	=	Laser Sheet Radius
r	=	Camera distance from scattering event
Re	=	Radius of Earth
σ	=	Stefan-Boltzmann Constant
T	=	Period
TC	=	External Temp
θ	=	Angle of View of Pixel
V	=	Relative Veloicty of Debris

I. Overview

A. Introduction

In 1957, Sputnik I became the first man made satellite to orbit Earth, marking the beginning of a new era. Since then, humans have continued to send objects into Earth orbit at a growing rate. These objects serve a variety of purposes, from observation of other countries to providing communication networks on a global scale. As sending objects to space became more commonplace, so did collisions among these objects. Beginning in the 1970's, the Soviet's Istrebitel Sputnik program created impactor satellites with the purpose of colliding with target satellites.[1] This program marked the first of many satellite collisions. Whether intentional or not, the result of satellite impacts are innumerable pieces of debris added into orbit. The debris can be potentially catastrophic to future missions and as a result require tracking.

Great efforts in improving debris tracking have been made by NASA. They are currently capable of tracking about 500,000 objects, all of which are the size of a marble or larger. However, there are still millions of untracked debris that remain in orbit due to their small size.[2] According to MIT, even a 1.3 mm object traveling at a typical relative impact velocity of 10km/s has the equivalent destructive power of a 0.22 caliber bullet fired from a long rifle.[3] Much of this space debris is accumulating around satellite-occupied regions of Low-Earth Orbit (LEO) at an exponential rate. This presents a set of risks to human spaceflight and space-based communications which will become unacceptable as these capabilities become more important to global society. For this reason, it is imperative that this problem be addressed in the immediate future.

B. Mission Imperative

We propose a satellite equipped with instruments designed to detect space debris down to a size of 1mm in diameter that resides in commonly occupied orbits. This satellite would then communicate this data to the ground where it will provide a more accurate and inclusive map of debris and could be used to mitigate the risk of collision with debris in future launches. As this technology continues to develop further, it could be used to fully map all debris in low earth orbit, which could eventually pair with other systems that would deorbit the more dangerous pieces of debris and

provide a net negative contribution to the layer of space debris.

The primary goal of SWEEP is to provide a technical demonstration of how a spacecraft can map the position and velocity of space debris more accurately than the current systems and relay the information to ground systems, mitigating the risk of in-flight collisions with debris for future spacecraft.

C. Literature Review

Current technology in space debris tracking provides a lot of useful data, but there are still clear areas for advancement. The majority of orbital debris tracking is made using ground based telescopes using optics, lidar, and radar. One major site was the NASA Orbital Debris Observatory which made use of a 3 meter liquid mirror telescope to perform debris tracking on objects as small as 1 cm.[4] Another widely used site was the ESA's FGAN Tracking and Imaging Radar. With it's 34 m diameter parabolic dish, the TIRA can detect debris as small as 2 cm up to 1000 km altitude.[5] Space based debris tracking is another area that has been looked into, albeit with much more primitive methods. One such method is estimating debris flux by measuring impact craters on a craft. A notable experiment using this method was the Mir Environmental Effects Payload (MEEP) from NASA, which used an aerogel material to capture and hold debris upon impact.[6]

Based on the previous available instruments and the data they were able to receive, there is a clear need for our proposed instrument. As mentioned earlier, these ground based instruments were only able to track debris down to 1 cm at the smallest. This also came at the cost of having massive instruments to track these particles. Space based flux estimation only provides a guess as to how much debris is out there rather than a solid number and trajectory information. Our SWEEP instrument will be able to obtain the information necessary to track the trajectory and size of particles down to 1mm, of which millions of particles currently remain untracked.

D. Trade Studies

In order to choose a spacecraft configuration that would be best suited for our mission requirements, a trade study was made to compare which payload could be used to track the debris. Eight critical characteristics were determined, each assigned a weight indicating their importance and relevance to the system. Another value was assigned to track how well each payload would meet the selected characteristics. A Fibonacci sequence scale from 0 to 21 was used to indicate how well each payload performed and fit the selected characteristics. For the payload selection Accuracy, Power, Mass, Range, Ease of Use, Reliability, and Cost were all considered areas in which we would score among the different potential systems. The order of weight was listed from highest to lowest in the previous sentence. The three payloads that were or interest included radar, the laser disk system, and optics. Accuracy in this case was given the highest weight because our main goal is to detect objects 1 mm and greater. Power was given the next greatest weight as it has the ability to drive the size of the entire spacecraft. Similarly mass was given a high weighting due to its trickle down effect on various systems of the spacecraft. The trade table is found below. Compared to radar, the laser disk system was ultimately chosen due to its high accuracy, and detail.[7] Comparing the laser disk system to optics, it was ultimately chosen due to accuracy and reliability over cameras.[8]

Table 1 Alternative System Trade Study

	Weight	**RADAR**	**Laser Disk**	**Optics**
Power	21	21	8	13
Mass	17	13	21	8
Range	13	1	13	5
Cost	6	8	8	5
Reliability	8	8	13	13
Accuracy	25	10	13	3
Ease of Use	10	1	13	8
Score	**100**	**1047**	**1301**	**763**

The second trade study looked at potential altitudes we could send the spacecraft to. The categories we evaluated were density, target size range, traffic, ease of insertion, drag, and eclipse time. These categories listed are in order of

weight from high to low. Density and target size range were given the highest weight because these categories would give the highest chance of a positive detection in our size range. Traffic was given the second highest weight as placing our craft into more common orbits would prove greater benefit to other craft, should we detect debris. Altitudes of 500 km, 750 km, 900 km, 1500 km, and 2000 km were all possible choices. An altitude of 900 km was ultimately chosen due to high debris density and target size range.[9]

Table 2 Parking Altitude Determination

Priority Altitude	Weight	500 km	750 km	900 km	1500 km	2000 km
Traffic	20	5	8	13	13	21
Density	25	5	13	21	13	8
Target Size Range	25	13	13	21	13	8
Ease of Insertion	10	21	21	13	5	3
Drag (J2, atm)	10	1	5	13	21	21
Eclipse Time	10	5	8	13	21	21
Score	**100**	**39**	**54**	**80**	**65**	**60**

II. Critical Design Documentation

A. Top-Level Requirements

After selecting an initial concept that provided a solution to the mandate, a set of mission objectives were generated to ensure the group stay on track. These top level requirements defined the fundamental goals of the project and clearly defined how to reach them. These mission objectives will be listed in the next table, and the derived Subsystem Requirements can be found in the Appendix.

Table 3 Mission Objectives

No.	Requirement	Rationale	Required Value	Expected Value	Verification Method
MO-1.1	Shall track position and velocity of space debris sized 1mm or larger in a 900 km orbit	By tracking position and velocity of debris not detectable from ground stations, SWEEP can provide a more accurate and inclusive debris map.	900 km orbit	900km Circular Orbit 63.4 degrees of inclination.	Demonstration
MO-1.2	Shall have 5-year mission life	A five year mission life provides enough time to provide complete debris mapping.	5 Years	10 Years	Analysis
MO-1.3	Shall downlink relative debris data to Johnson Space Center.	Ground Stations will be able to spare the computational power to calculate the trajectories of the Debris	Downlink 10MB every orbit	Downlink 10.8MB every orbit	Analysis
MO-1.4	Shall deorbit at the end of mission life.	One of the main objectives of SWEEP is to have a net positive effect on Orbital Debris.	252 m/s	252 m/s	Analysis
MO-1.5	First operational satellite shall be launched no later than January of 2025.	As space travel in the vicinity of earth becomes more commonplace we will need a better understanding of the presence of debris.	January 2025	January 2025	Analysis

B. Concept of Operations

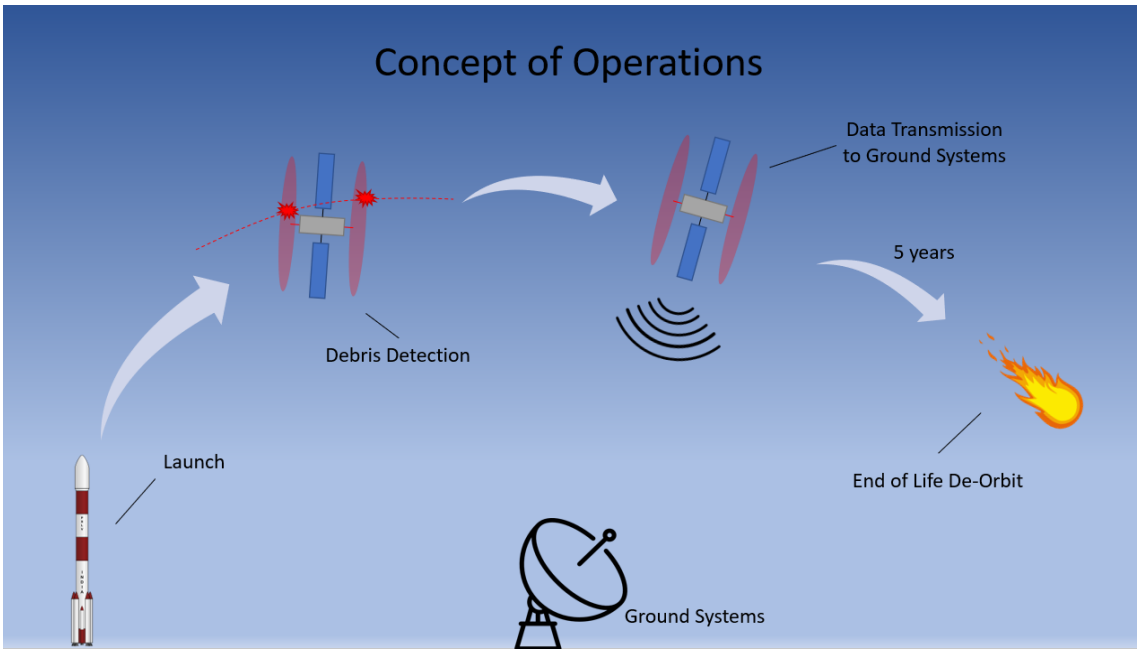

From the mission objectives and the derived requirements a concept of operations was derived:

1) The SWEEP system is launched into its orbit
2) SWEEP detects orbital debris recording debris' velocity vector as well as the attitude and orbital parameters of SWEEP
3) This data is then transmitted to the ground station when visible
4) The data is processed on the ground to calculate the debris orbital parameters
5) At the end of the mission, SWEEP will be deorbited

The details of SWEEP's subsystems which are required to carry out its mission are outlined in the following sections.

C. Subsystems

1. Payload (Debris Detection and Tracking System)

The tracking of measured debris relies on the position and velocity of the debris relative to the spacecraft as well as the position and velocity of the spacecraft in an Earth-Centered Inertial (ECI) reference frame. The purpose of the payload is to determine the velocity and position of the debris relative to the spacecraft, and the method selected was outlined in Optical Orbital Debris Spotter(OODS) authored by Chistopher Englert of the Naval Research Laboratory[10]. OODS describes a method for measuring debris flux with a single small 1 meter disk for debris sizes 1.0 to 0.01cm. This method uses a laser that is pointed at a conic mirror to diffuse the laser into a disk. As the spacecraft travels through its orbit, it will sweep out an area where there is expected debris. As the debris crosses this disk, the light from the laser will be scattered and this scattering event will be captured by a camera. OODS also states that the size of debris can be estimated given the angle of scattering event, location on disk, and amount of light detected.

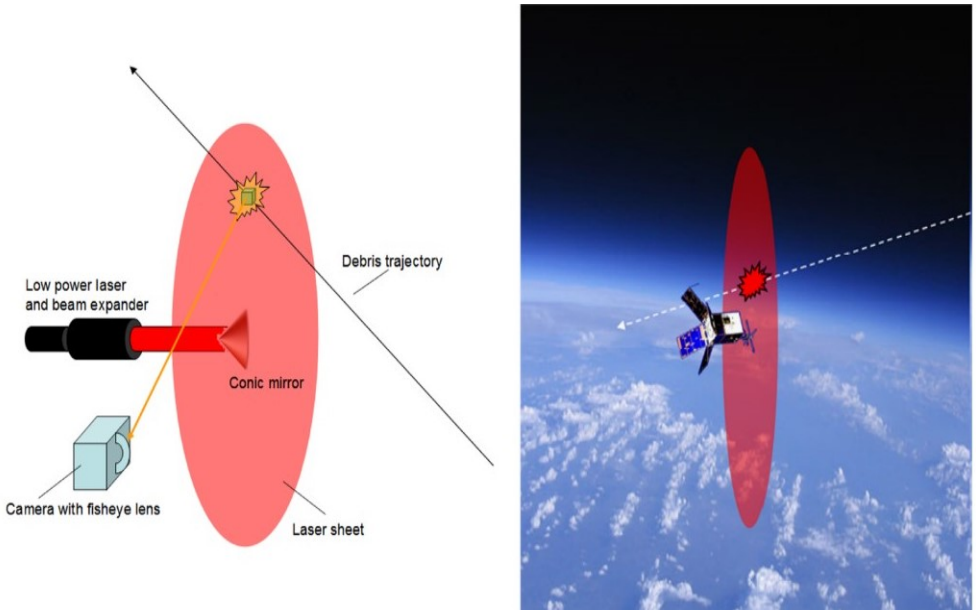

Fig. 1 Illustration of the OODS Flux measurement Method

This method allows for the measurement of position relative to the spacecraft but not velocity, to do this it was determined that using two disks would be required to measure the velocity vector of debris by determining the position at the two disks and the time between intersections. The method addressed in this paper will be capable of measuring 1mm and greater objects with relative speeds of 15 km/s.

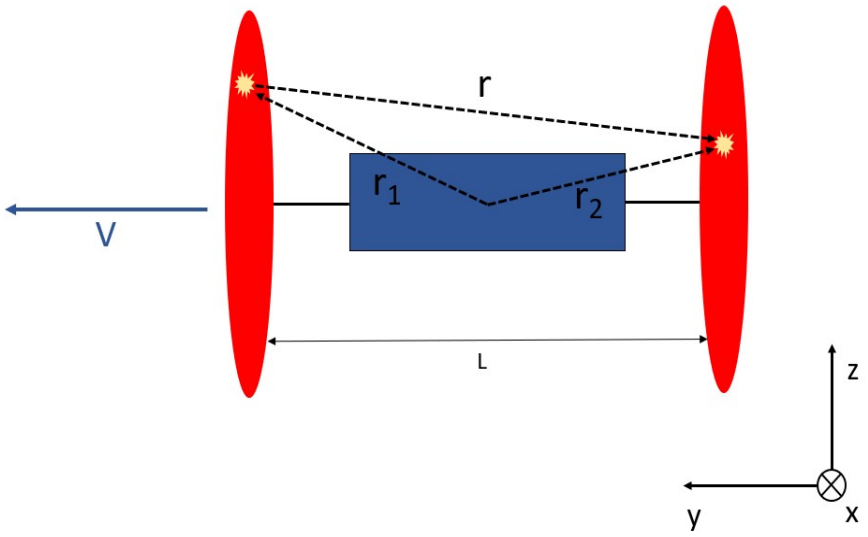

Fig. 2 Illustrated Detection Event

The laser-disk described in OODS also was only a meter in radius which would yield a very small amount of flux. To increase the area that is swept out over the same period of time, the radii of the disks were increased which requires a higher power laser than the mW range laser mentioned in OODS. It was determined that a disk with a radius of 500m would give a sufficient amount of debris interactions.

Laser

Wavelength: The selection of the laser was primarily driven by the wavelength, due to the importance of limiting the sensor noise from the sun and increasing the amount of expected photons returned from the detection event. From Fig. 3 it is shown that the radiative flux approaches zero as the wavelength increases and can be assumed zero for wavelength > 3000 nm. Having a laser with a wavelength greater than this is ideal to minimize the noise from the sun[11]. An equation in OODS describes the effect of wavelength (shown in next section) and how the optical power is inversely proportional to the wavelength. From these two factors it was easily determined that the laser should be within the IR band. Ultimately, a laser with a wavelength of 10600nm was selected as it minimizes the optical power, maximizes the number of photons that reach the sensor, and is relatively common for industrial lasers.

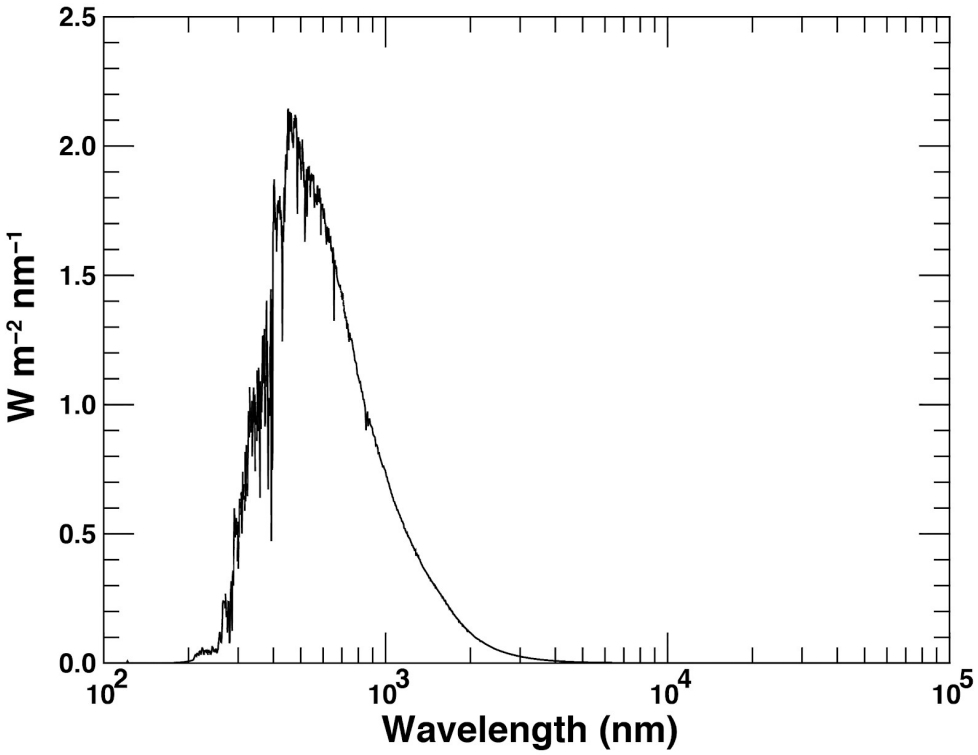

Fig. 3 Solar Spectral Irradiance

Laser Optical Power: The optical power was calculated using the equation described in OODS. This calculation can be seen below.

$$N = Number\ of\ Photons = 100$$

$$A = Camera\ Aperture\ Size = 1cm^2$$

$$L = Size\ of\ Detectable\ Debris = 1mm$$

$$\lambda = Laser\ Wavelength = 10600nm$$

$$h = Planck\ Constant = 6.62607 * 10^{-34} m^2 kg/s$$

$$c = Speed\ of\ Light = 299,792,458 m/s$$

$$R = Laser\ Sheet\ Radius = 500m$$

$$r = Camera\ distance\ away\ from\ scattering\ event = 500m$$

$$V = Relative\ Velocity\ of\ Debris = 10km/s$$

$$N = \frac{PAL^2\lambda}{4\pi^2 hcvRr^2}$$

$$P = \frac{4\pi^2 hcvRr^2 N}{AL^2\lambda}$$

$$P = \frac{4 * \pi^2 (6.62607 * 10^{-34} m^2 kg/s)(299,792,458 m/s)(10 km/s)(500m)(500m)^2 * 100}{(1cm^2)(1mm)^2(10600nm)}$$

$$P = 92.5W per orbital debris sensor$$

Accounting for losses in the laser disk system(e.g. Mirror, Filters, sensor, etc.) the optical power is increased to 100 W.

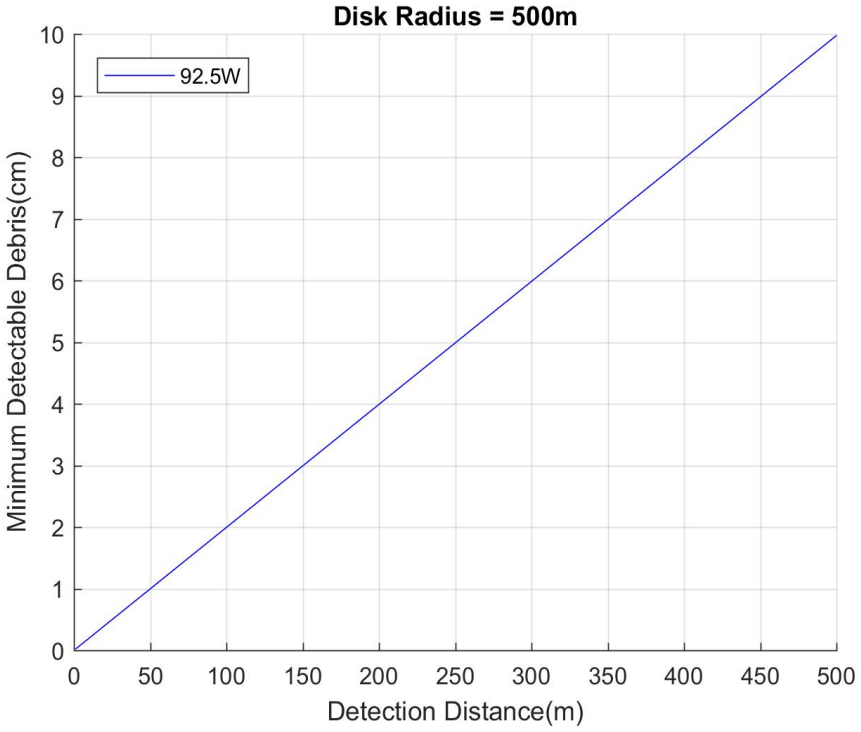

Fig. 4 Range of Detection for Debris Sizes

Estimated Laser System Power: To estimate the power required to run a laser with a wavelength of 10600nm and optical power of 100W, the input powers of lasers of the same wavelength were plotted over a range optical powers. A curve was then fitted to the data so the estimated power could be found, yielding 1360W[14].

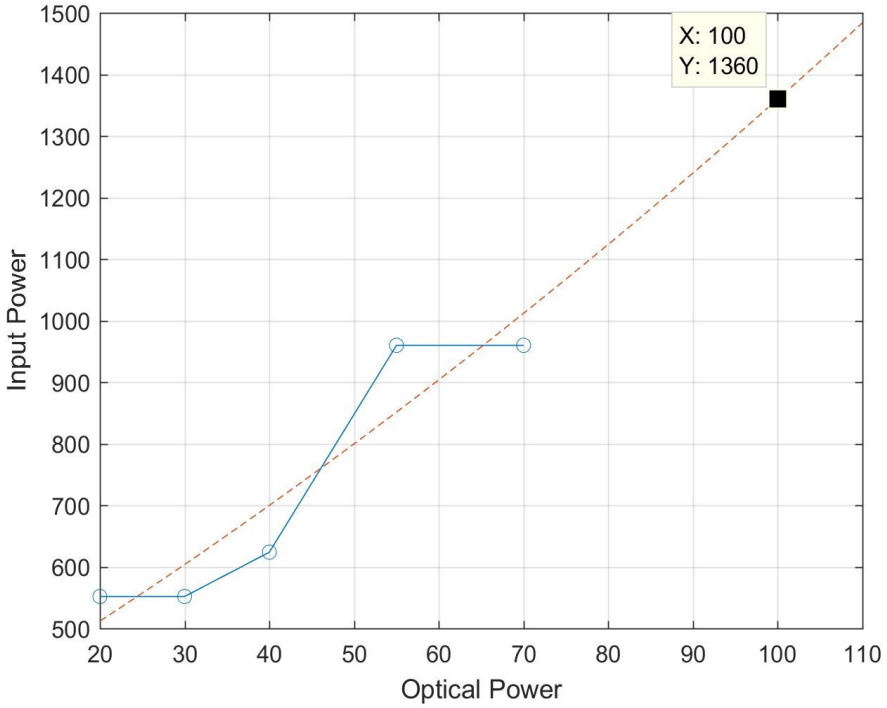

Fig. 5 Input Power vs Optical Power Plot

Conic Mirror: In order to transform the laser beam into a disk, the laser must strike a conic mirror at a 45° angle as shown in Fig. 6. Gold coating was selected for the conic mirror as it has reflectance of 98% at with range of 2,000-12,000nm[15, 16].

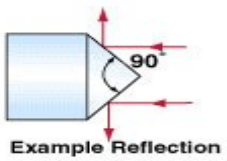

Fig. 6 Conic Mirror Example

Sensor (Thermal Optic)

Sensor Overview: To determine the location and time a piece of debris intersects each disk, sensors will be required to monitor the full area of both disks. This system of sensors will be looking for the reflected laser light off of debris and reporting the location and time of intersection on the disks, as well as the intensity (brightness) of the reflection. This data will then be sent to the ground stations where the size of the debris and orbital elements of debris can be calculated.

Focal-Plane Array(FPA): A low noise sensor will be required to distinguish the signal due to the small amount of photons being reflected back to the sensor, which is a function of distance, size, and speed of debris. Consequently, a Charged-Coupled Device (CCD) was selected because they produce lower noise when compared to a CMOS FPA and generally produce higher quality images.

To adequately measure the position of the debris crossing the laser disk, the pixels on the cameras must have an adequately small footprint on the disk. To determine the number of pixels required the pixels are assumed to be evenly

distributed within the optics projected cone. The equations used are shown below:

$hn = Corresponding\ Pixel\ Height$
$N = Number\ of\ Pixels$
$\theta = Angle\ of\ View\ of\ Pixel$
$\gamma = Angle\ from\ Center - Line$
$HFC = Height\ from\ Center - Line$

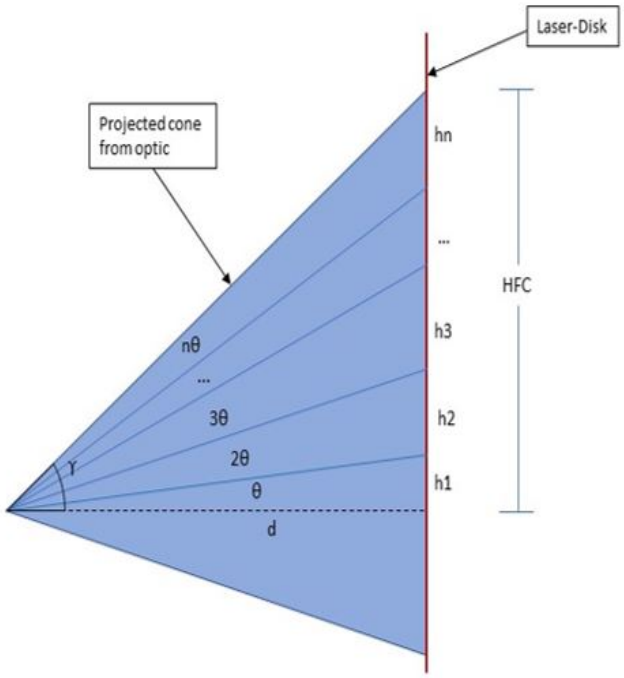

Fig. 7 Illustration of pixel distribution over laser disk [10]

From Geometry:

$$\theta = \frac{\gamma}{N}$$

$$h(1) = dtan(\theta)$$

$$h(n) = dtan(n\theta) - \sum_{n=1}^{N} h(n-1)$$

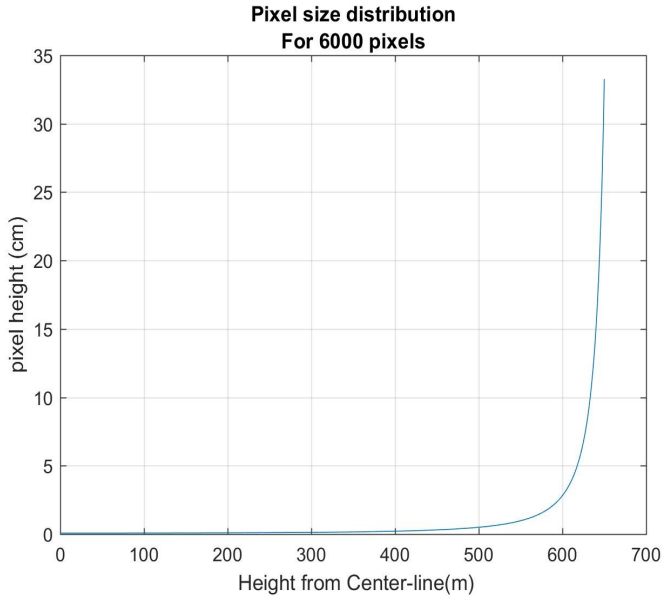

Fig. 8 Plot of pixel height vs. vertical distance

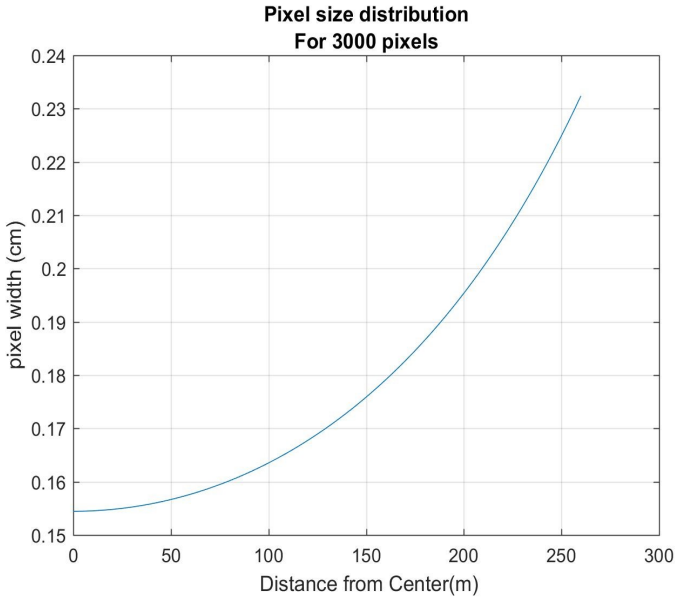

Fig. 9 Plot of pixel width vs. horizontal distance

From these equations at the maximum height of 500 m, the pixel-height is found to be 0.50 cm for a column of 6000 pixels. The pixel-width at the maximum width of 225m, was shown 0.21cm for a row of 3000 pixels (the maximum values are for the 8-camera configuration shown below Fig. 11). This yields a FPA size of 6000x3000 pixels.

Sampling Frequency: The sampling frequency is critical as knowing the exact time the debris crosses each disk is the only way to calculate debris velocity. To determine the sampling frequency, the transit time of an object the minimum required size and maximum required velocity must be calculated. To make this calculation, assume a 1mm cube traveling at 15km/s passes through the disk for simplicity. Using these parameters, one image is required to be taken every 66 ns to capture the debris while it is in the plane of the disk. However, it is important to keep in mind that

the Field of view (FoV) of the sensors are overlapping close to the spacecraft(Fig. 11). If there are three overlapping sensors and they are synchronized such that there will always be one camera looking at the area with an open lens, the sampling rate can be reduced to one image per 200ns, 5 MHz or 5 million frames per second. Such a high number of images per second poses a significant issues on data storage and processing, this will be addressed in later sections of this report.

Filter: A filter is required to eliminate any wavelengths not the same as emitted by the laser to reduce noise. The selection for a filter was driven by two characteristics: a high transmittance at the selected wavelength of 10650nm and having as narrow a band as possible to reduce noise to the sensor. The selected filter has 92% at 10650nm and band width 11.37%[13]

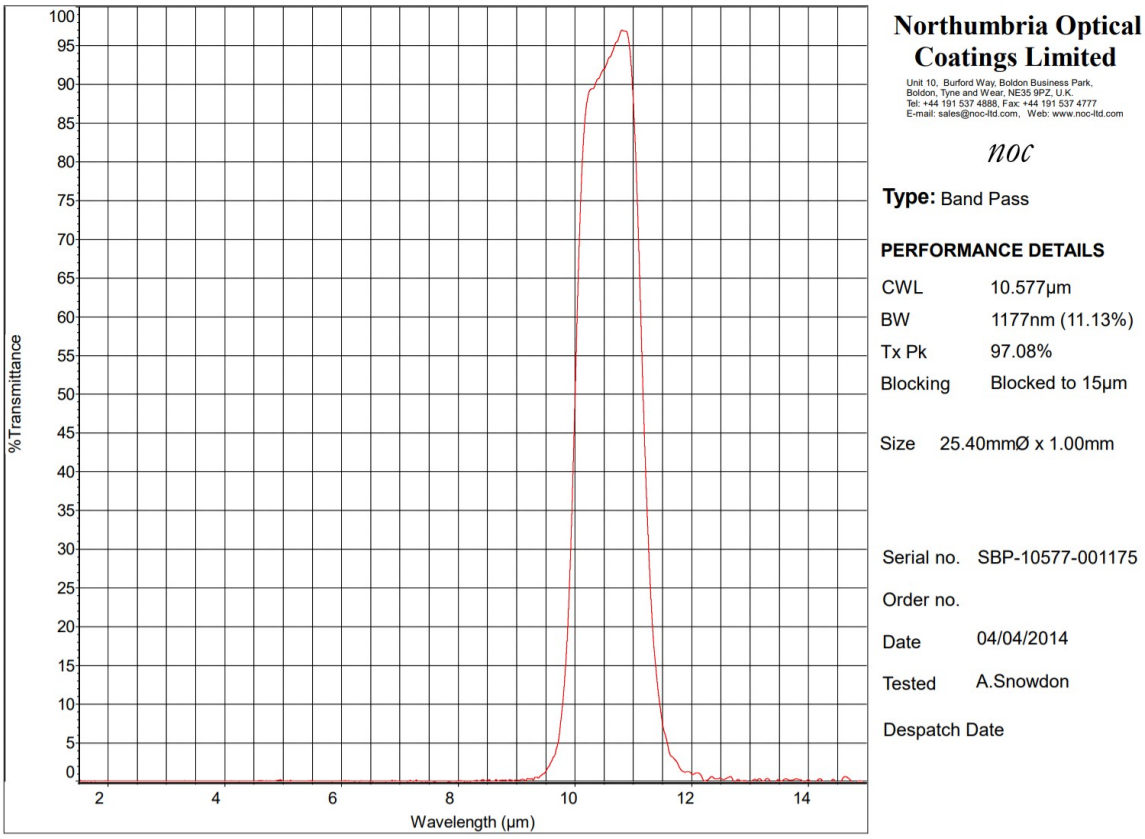

Fig. 10 Percent transmittance of selected filter vs. wavelength

Lens: The primary drivers for the lens selection is the Angle of View (AoV) and insuring that entire FoV is in focus. To maximize the FoV, the AoV would ideally be 180°, or as large as possible. For the entire image to be in focus, the hyperfocal distance must be lower than the distance from the FPA to the disk (1.5m). Conveniently, the hyperfocal distance for wide-angle lenses is generally much lower than this. For example a Rokinon 7.5mm f/3.5 has an angle of view of 180°and a hyperfocal distance of 23.6mm[12]. A lens with germanium (High IR transmission) elements with similar geometry to the Rokinon would be ideal for these sensors.

Sensor Configuration on Spacecraft: To determine the number and configuration of the optics required for full coverage on the laser-disk, each sensor's field of view (FOV) must be calculated.
$AoV = Angle\ of\ View$
$AFC = Angle\ From\ Center$

$DiskRadius = 500m$

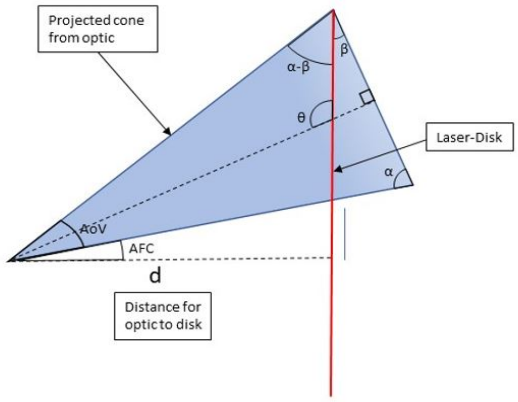

Fig. 11 Geometry of optics for Field of View Calculation

From Geometry:

$$\alpha = \frac{180 - AoV}{2}$$

$$\beta = AoV + AFC + \alpha - 90$$

From these angles the eccentricity can be solved:

$$Eccentricity(e) = \frac{sin\beta}{sin\alpha}$$

$$SemiMajor\ Axis(a) = 500m - dtan(AFC)$$

$$SemiMinorAxis(b) = a\sqrt{1 - e^2}$$

After the parameters of the ellipses are calculated it was then plotted around the disk such that the entire laser-disk area is fully covered by sensors. A variety of configurations are possible by varying AoV, Number of sensors, and top of FoV.

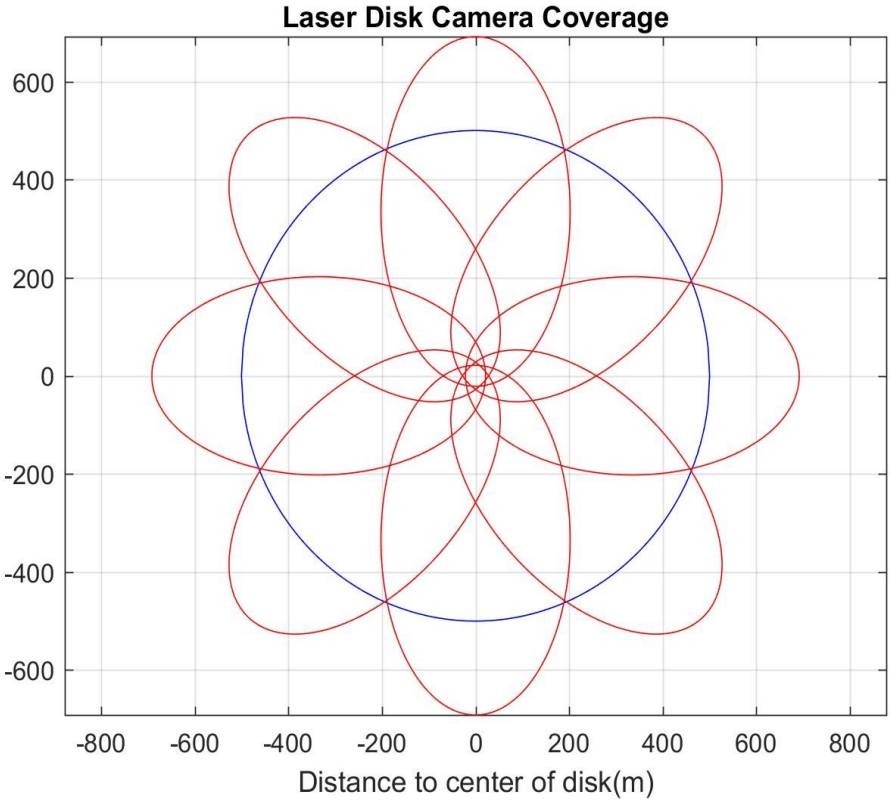

Fig. 12 Eight camera configuration. *Sensor's Field of View (Red) and Laser-Disk (Blue).*

Frequency of Debris Encounter: SWEEP's target size range is centered around 1mm to 10cm objects. Trade studies that the team has conducted along with evidence from reports written by NASA the ESA and SMAD all provide data showing that the density of objects within this size range experiences its peak within the altitudes of 800km to 1000km. This also happens to be just outside the limits of distance and altitude that powerful ground radar stations are capable of observing. This creates a special niche for SWEEP's mission.

> *"Such objects, however, can generally not be correlated with specific launch events, nor can their orbits be determined with sufficient accuracy to be predictable in future." (European Space Agency, Jan 24th, 2018)*

Going off of this target size range, the team wanted to identify what the flux of this debris range would be at 900km (Our parking orbit). Multiple graphs were discovered that provide estimates for this number.

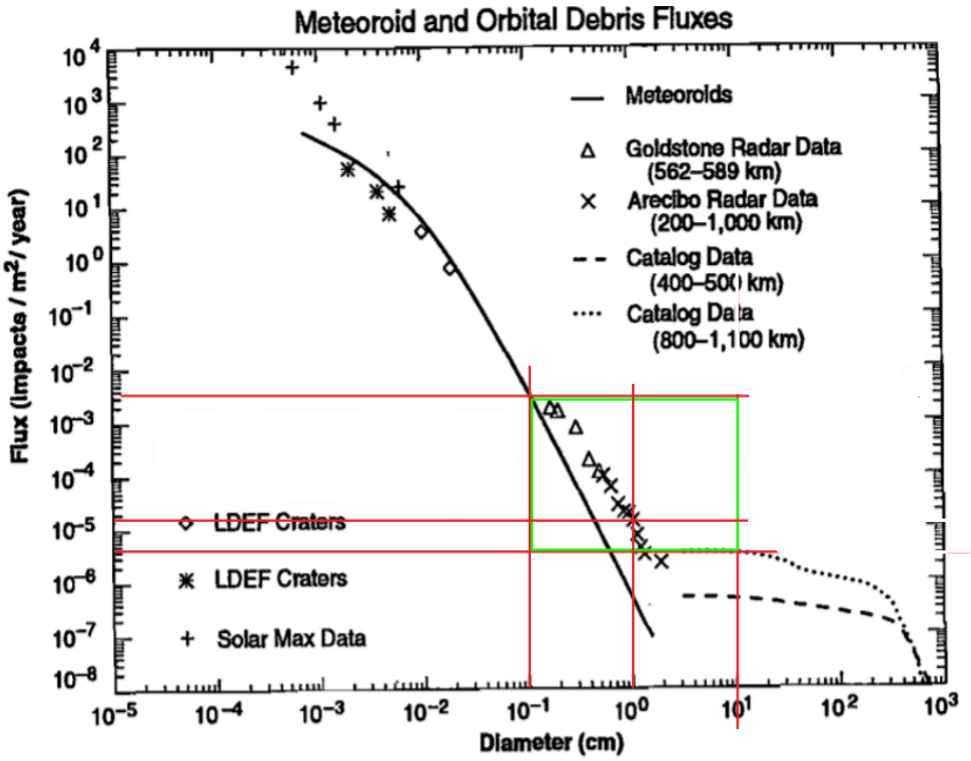

Fig. 13 Meteorite and Orbital Debris Fluxes

The average density of these objects is reported by SMAD to be $10^{-8} km^{-3}$.

"The density of tracked objects peaks at 4 x 10-8 objects per cubic kilometers at 850 km altitude." (Craft, Brane, NASA, February 1st, 2017)

This very helpful graph shows the flux of variously sized space debris, the altitude at which it was found, and the type of instrument that was used to observe it. Using this plot the team wanted to identify the region of this graph that the the SWEEP project would be shedding light upon. In this plot, the green square encompasses the target range of the Sweep mission. Using this data team team was able to determine the frequency at which object would be passing through different sections of the disc. Remember that the laser disc mirror setup enables SWEEP to detect 1mm objects out to 5 meters away, 1cm objects out to 50 meters away,and 10cm objects at 500 meters away from the craft. Keep in mind however that SWEEP will be able to detect objects that are even larger than 10 cm in size if they were to pass through the laser disc. This means that there was no upper size limit set in the flux calculations.

Performing a sample calculation for a 1cm particle, the $impacts/m^2/year$ is given as $10^{-4.9}$ and a maximum detection radius of 50 m. The impacts per year can then be found as shown below.

$$\left(10^{-4.9}\frac{\sqrt{impacts/m^2}}{year}\right) * \left(\pi * 50^2 * m^2\right) = 0.0785\frac{impacts}{year} = 0.00027\frac{impacts}{day}$$

The following values were then calculated using the same method.

Table 4 Occurrence of Debris Detection

Debris Size	Detectable Radius (m)	Detectable Area (m^2)	Flux (No/m^2/year)	Impacts/Day
1 mm	5	78.54	10e-2.7	4.29e-04
1 cm	50	7853.98	10e-4.9	2.71e-04
10 cm	500	785398.16	9.66e-06	2.08e-02
			Total:	0.0215

This works out to be approximately one guaranteed impact of any size every 47 days. Due to the small amount of data representing this size of debris at the target altitude, these values are only an estimate. This data also enables the team to develop a unique plot that displays the total flux of debris throughout the different regimes of the detection plane. As can be seen in the logarithmic plot below, the maximum total flux can be expected out at the furthest point away from the mirror.

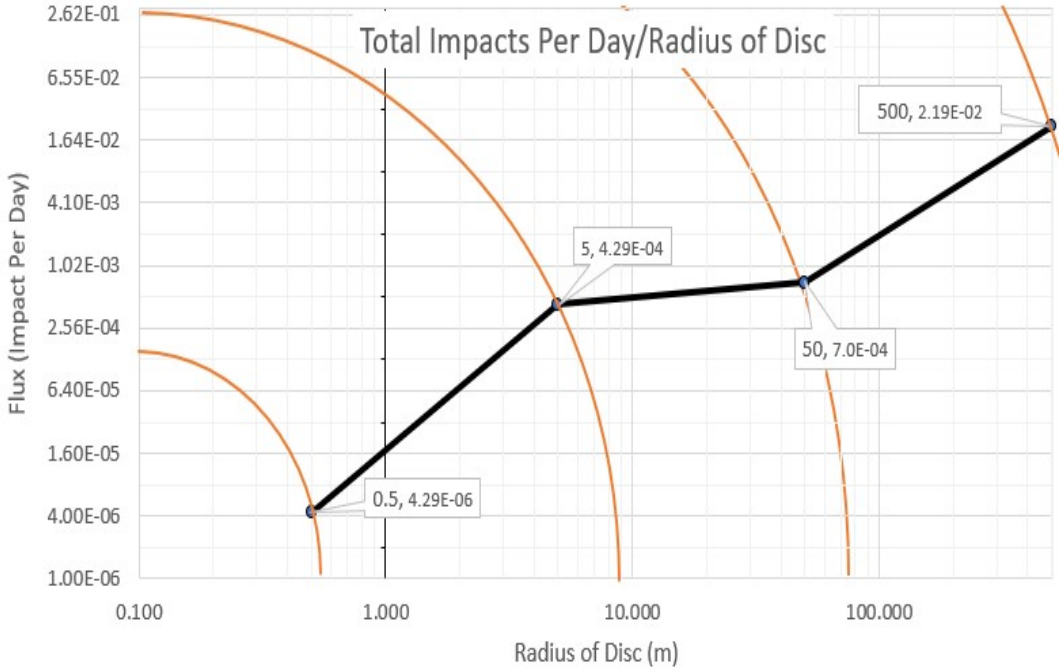

Fig. 14 Total Impacts Per Day/Radius of Disc

2. Orbital Conditions and Determination

The orbital conditions for the SWEEP spacecraft were determined based on current satellite and debris populations and their respective densities. It it is critical to occupy an orbit that is both useful to future spacecraft and is of sufficient density of debris to establish a meaningful dataset.

As shown in Fig. 15, most spacecraft currently reside in orbits with perigee and apogee at around 900 km. This asserts that most current orbits are also circular. Figure 16 supports this argument as it is shown that 74% of the current catalog of satellites reside in an orbit eccentricity of less than 0.1. The following information references the Fundamentals of Astrodynamics.[43]

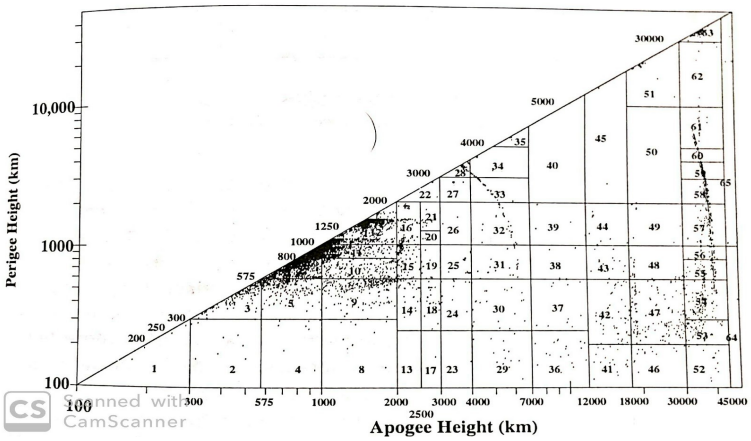

Fig. 15 Orbital Density

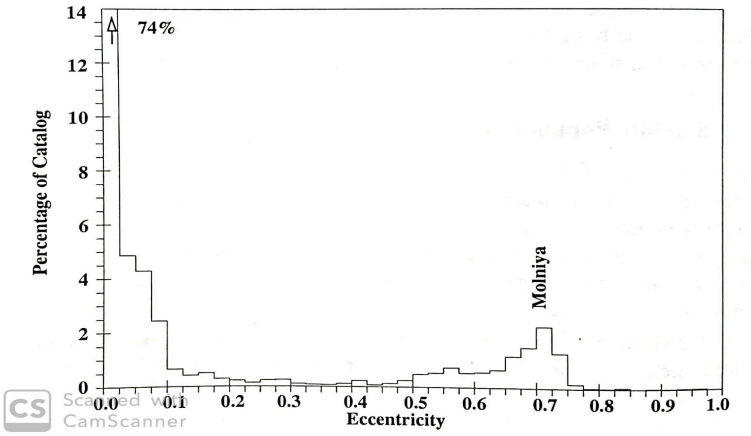

Fig. 16 Eccentricity vs Percentage of Catalog

The highest populated inclination, as shown in Fig. 17, is slightly more complicated. It can be seen that most spacecraft inhabit three specific inclinations - The "critical" Inclination as well as the polar and sun-synchronous regions. Critical inclination is a region in which J2 perturbation is minimized, reducing apogee drift due to the oblateness of the Earth. Polar inclination is as the title suggests, an inclination in which the spacecraft will pass over the poles of the Earth, and a sun-synchronous orbit is one that retains a spacecraft in constant daylight.

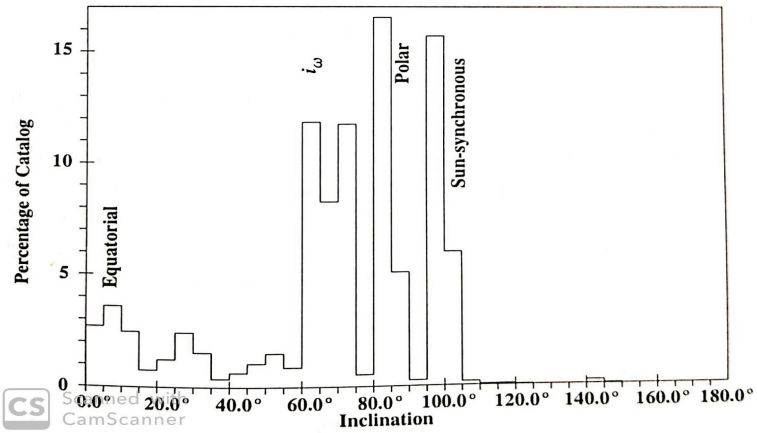

Fig. 17 Inclination vs Percentage of Catalog

Although it is not the highest populated inclination, an orbit with a critical inclination of 63.4°was selected in order to reduce required velocity changes for station keeping and the inherent weight associated with that.

Our spacecraft may be very power-hungry, however, it was determined that larger batteries in a critically inclined orbit will be more effective than a sun-synchronous orbit in which we may receive more sunlight for our power system, but will have to carry more fuel in order to account for a more intense station keeping regiment.

Based on the data above, these conditions will best serve future spacecraft if the current trend continues. The following orbital parameters have been selected:

$$a = 7,278km$$

$$e = 0$$

$$i = 63.4^\circ$$

$$\omega = 0^\circ$$

$$T = 102.988min$$

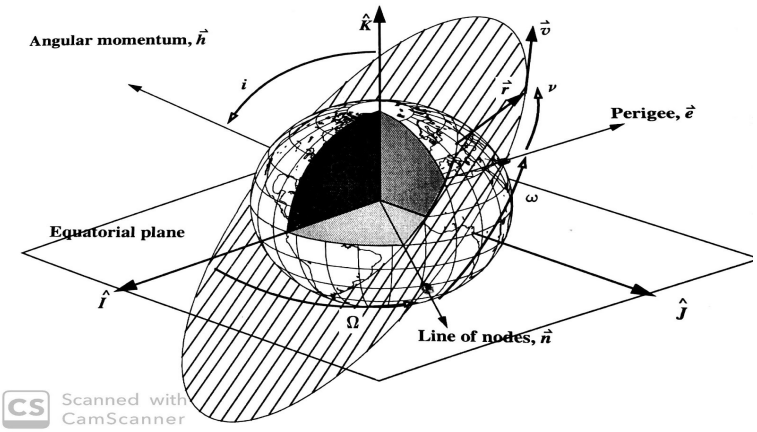

Fig. 18 Orbital Elements

Orbit Perturbation Analysis [42]

1) Third-Body Perturbations
The SWEEP spacecraft will not only be subjected to the gravitational forces of the Earth but to those of the sun and moon as well. These forces affect all orbital elements periodically, however, have the greatest secular effects on right inclination and argument of perigee. Orbital precession rate can be approximated using the following equations:
Right ascension of the ascending node :

$$\dot{\Omega}_{Moon} = -0.00338(cos(i))/n$$

$$\dot{\Omega}_{Sun} = -0.00154(cos(i))/n$$

Argument of perigee :

$$\dot{\omega}_{Moon} = 0.00169(4 - 5sin^2(i))/n$$

$$\dot{\omega}_{Sun} = 0.00077(4 - 5sin^2(i))/n$$

Where i is the orbital inclination and n is number of orbit revolutions per day. Both values are in degrees per day and do not take into account the changing orientation of the orbital plane with respect to the orbital plane of the moon or the ecliptic plane. For the spacecraft, because we will be critically inclined, changes in argument of perigee will essentially be 0 deg/day.

2) Non-Spherical Earth Perturbations
Although many times it is modelled as a perfect sphere, the Earth actually bulges toward the equator. This causes variation in gravitational effects that inherently affect the orbit of the spacecraft. Again, most significant secular effects occur in right ascension and in argument of perigee.

$$\dot{\Omega}_{J_2} = -1.5nJ_2(R_E/a)^2(cosi)(1 - e^2)^{-2}$$

$$\dot{\Omega}_{J_2} \approx -2.06474 * 10^{14}a^{-7/2}(cosi)(1 - e^2)^{-2}$$

$$\dot{\omega}_{J_2} = 0.75nJ_2(R_E/a)^2(4 - 5sin^2 i)(1 - e^2)^{-2}$$

$$\dot{\omega}_{J_2} \approx 1.03237 * 10^{14}a^{-7/2}(4 - sin^2 i)(1 - e^2)^{-2}$$

Where n is mean motion in deg/day, Re is radius of the Earth at the equator, a is semimajor axis of the orbit in km, i is the orbital inclination and e is the eccentricity of the orbit.

3) Drag Perturbations
Spacecraft in LEO are subjected to atmospheric drag. This perturbing force acts opposite the velocity vector and causes orbit to decay over a period of time. Unfettered, this force would eventually cause our spacecraft to plunge back into the Earth. This deceleration (for a circular orbit) can be approximated as follows:

$$\Delta a_{rev} = -2\pi(C_D A/m)\rho a^2$$

$$\Delta P_{rev} = -6\pi^2(C_D A/m)\rho a^2/V$$

$$\Delta V_{rev} = \pi(C_D A/m)\rho aV$$

$$\Delta e_{rev} = 0$$

Where Cd is drag coefficient, A is cross-sectional area, m is mass of the spacecraft in kg, is air density, P is orbital period, and V is satellites velocity with respect to the atmosphere. Each value is given per revolution.

4) Solar Radiation
Solar radiation pressure can be approximated using the following equation.

$$a_R \approx -4.5 * 10^{-6}(1 + r)A/m$$

Where A is cross-sectional area exposed to the sun in square meters, and m is satellite mass in kg. This acceleration is related to the reflective factor r in which a spacecraft with $r = 0$ absorbs all incoming radiant energy, and a spacecraft with $r = 1$ reflects all incoming radiant energy.

Orbital Calculations For a circular orbit with an altitude of 900km, the period can be calculated as follows.

$$R = 6378km + 900km = 7278km$$
$$\mu = 3.986 * 10^{14} m/s$$
$$T = 2\pi\sqrt{\frac{R^3}{\mu}}$$
$$T = 2\pi\sqrt{\frac{7278100^3}{3.986 * 10^{14}}} = 6179.28sec = 102.988min$$

Third Body Perturbations

$$i = 63.4deg$$
$$n = 13.9825 revolutions\ per\ day$$

$$\Omega_{moon} = -0.000338cos(i)/n$$
$$\Omega_{moon} = -0.000108deg/day$$

$$\Omega_{Sun} = -0.00154cos(i)/n$$
$$\Omega_{Sun} = -0.0000493deg/day$$

$$\omega_{moon} = 0.00169(4 - 5sin^2 i)/n = 0$$
$$\omega_{Sun} = 0.00077(4 - 5sin^2 i)/n = 0$$

Non-Spherical Earth Perturbations

$$n = 0.00102deg/day$$
$$J_2 = 0.001082635$$
$$Re = 6378km$$
$$e = 0$$

$$\dot{\Omega}_{J_2} = -1.5nJ_2(R_E/a)^2(cosi)(1 - e^2)^{-2}$$
$$\dot{\Omega}_{J_2} \approx -2.06474 * 10^{14} a^{-7/2}(cosi)(1 - e^2)^{-2}$$
$$\dot{\Omega}_{J_2} \approx -2.811deg/day$$

$$\dot{\omega}_{J_2} = 0.75nJ_2(R_E/a)^2(4 - 5sin^2 i)(1 - e^2)^{-2}$$
$$\dot{\omega}_{J_2} \approx 1.03237 * 10^{14} a^{-7/2}(4 - sin^2 i)(1 - e^2)^{-2}$$
$$\dot{\omega}_{J_2} \approx 0deg/day$$

Drag Perturbations

$$C_D \approx 2.2$$
$$A \approx 12.25m^2$$
$$m \approx 340kg$$

$$\rho \approx 5.46 * 10^{-15} kg/m^3$$
$$a = 7278000m$$

$$\Delta a_{rev} = -2\pi(C_D A/m)\rho a^2$$
$$\Delta a_{rev} = -0.144m$$

$$\Delta P_{rev} = -6\pi^2(C_D A/m)\rho a^2/V$$
$$\Delta P_{rev} = -1.83449 * 10^{-4} sec$$

$$\Delta V_{rev} = \pi(C_D A/m)\rho a V$$
$$\Delta V_{rev} = 7.32261 * 10^{-5} m/s$$

$$\Delta e_{rev} = 0$$

Solar Radiation

$$r \approx 0.4$$
$$a_R \approx -4.5 * 10^{-6}(1 + r)A/m$$
$$a_R \approx -2.501 * 10^{-7} m/s^2$$

Table 5 Perturbation Summary

	Perturbation					**Total**
	Sun	Moon	J2	Drag		Over 5 years:
Degrees per day	Ω	-0.0000493	-0.000108	-2.811		-5130.4 deg
	ω	0	0	0		0 deg
Per Revolution	Δa_{rev}				-0.144m	3.674 km lost
	ΔP_{rev}				-1.83449*$10^{-4} sec$	4.68 sec lost
	ΔV_{rev}				7.32261*$10^{-5} m/s$	1.868 m/s lost

3. Launch Systems and Propulsion

In order to minimize the relative velocity between the debris and SWEEP, we have decided to launch into a prograde orbit. Launching into this particular orbit constricts us to using a launch site on the east coast of the United States to prevent a failed rocket from crashing into land. Launching into a prograde orbit also allows SWEEP to benefit from the earth's rotational velocity, reducing the delta-v required by the launch vehicle. The ideal launch site for SWEEP will be the Cape Canaveral Air Force Station at 28.5°latitude, providing the launch vehicle with an additional 407 m/s.

$$\Delta v_o = R_e * \omega * cos(\theta)$$
$$\Delta v_o = (6378km) * (7.27 * 10^{-5}\ rad/s) * (cos(28.5°)rad)$$
$$\Delta v_o = 407m/s$$

The purpose of SWEEP is to map debris in space, and it would be counter-intuitive to use a launch vehicle that produces debris in space. SpaceX is currently operating with a reusable first stage and deorbits its second stage by

ensuring its remaining fuel reserves can safely and intentionally decay its orbit. Because of this, we have decided to launch SWEEP using a SpaceX Falcon 9 Block 5. This is a two-stage launch vehicle capable of delivering a 22,800 kilogram payload to Low-Earth Orbit, which will far exceed our requirements. SpaceX also operates out of Cape Canaveral, removing the need to transport our spacecraft to a different location.

The initial driving factor behind the choice for the onboard monopropellant thrusters was the need for SWEEP to deorbit itself at the end of life, orbital station keeping, and the need to desaturate the reaction wheels. Early estimates for how much thrust the engines would need to output to desaturate were arrived at by observing what the FireSat mission would have had to use. The example calculations from SMAD, showed that the Firesat example mission would require .5 N to .8N of thrust to desaturate its wheels. However, a report prepared by Honeywell Inc, Satellite Systems Division showed that a vehicle with a mass of 500 kg would need to produce a moment of .1 Nm.

The team was aware that there were still some factors that had not yet been taken into account, such as environmental disturbances, factors of safety, and SWEEP's larger moments of inertia. The team was able to conclude that SWEEP would likely need more than .8N to desaturate. As a result, the team landed on the MR-111C 4N hydrazine monopropellant thruster. With this generous amount of thrust, the team will be able to satisfy the orbital requirements of PR-3.1 and PR-3.2.

The team was set on a specific desaturation thruster configuration, this layout was provided by "A Brief Survey of Attitude Control Systems for Small Satellites Using Momentum Concepts" as shown in Fig. 19. It depicts a total of six thrusters mounted on the vehicle. Four of these being aft translational thrusters (which would also be able to provide a small torque if need be, since they would have a moment arm l=.25m), as well as two rotational thrusters that would induce a moment about the x axis (roll) of the vehicle. Moving forward in the design process, the team was interested in conducting a thorough analysis on the exact power needed from the desaturation thruster. To do this, the team would have to conduct the same analysis that SMAD conducted. The calculations for this analysis span tables 19 to 23. Throughout this investigation it was shown that in order to overcome every external and internal torque that was produced, SWEEP would require 2.65N of thrust. This was good news, since it roughly corresponded with what the team had predicted. However, this began to raise concerns of whether or not it would be practical to continue to desaturate via thruster, or to switch to an alternative method for fuel savings. The findings of this investigation can be found in the Guidance, Navigation and Control Section.

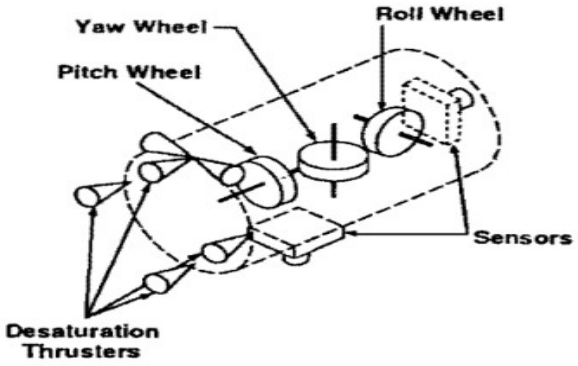

Fig. 19 Desaturation Thruster Configuration

Due to drag, J2 perturbations, solar radiation pressure, and tidal forces, SWEEP's orbit will begin to decay after being delivered. To prevent SWEEP's orbit from decaying, it must perform station keeping maneuvers to maintain its desired orbit of 900km altitude and 63.4° inclination one time each year. Each of these maneuvers will require 10 m/s of delta-v, summing to a total of 50 m/s of delta-v and 12 kg of hydrazine to maintain its orbit over the 10-year mission life.

One of SWEEP's mission objectives is to deorbit at end-of-life to prevent the spacecraft from remaining in orbit after it has completed its mission. Due to the small size of SWEEP, the spacecraft is expected to burn up in the atmosphere in response to extreme frictional forces. However in the very miniscule chance that the spacecraft survives re-entry, SWEEP will be aimed to land in the spacecraft cemetery located in southern Pacific Ocean. This location is the point on Earth farthest from land and is home to more than 200 spacecrafts that have been deorbited. The deorbiting process will be done by performing a single Hohmann transfer from our orbit at 900km altitude to the surface of the earth, requiring a total of 252 m/s of delta-v and 56 kg of hydrazine. This transfer will take approximately 47 minutes to complete.

$$\Delta v_{deorbit} = \left| \sqrt{\frac{\mu}{r_1}} * \left(\sqrt{\frac{2r_2}{r_1 + r_2}} - 1 \right) \right|$$

$$\Delta v_{deorbit} = \left| \sqrt{\frac{398600km^3/s^2}{7278km}} * \left(\sqrt{\frac{2 * 6366km}{7278km + 6366km}} - 1 \right) \right|$$

$$\Delta v_{deorbit} = 252m/s$$

$$\Delta t_{deorbit} = \pi * \sqrt{\frac{(r_1 + r_2)^3}{8\mu}}$$

$$\Delta t_{deorbit} = \pi * \sqrt{\frac{(7278km + 6366km)^3}{8 * 398600km^3/s^2}}$$

$$\Delta t_{deorbit} = 2803.8s = 46.7min$$

The station-keeping maneuvers and deorbiting process will require a total of 68 kg of hydrazine. The density of hydrazine is 1020 kg/m^3, so we will need 66.67 liters of hydrazine for the mission. Northrop Grumman Part Number 80364-1 is a fuel tank capable of holding 91.44 liters of fuel and will be used to store SWEEP's propellant. An added benefit of selecting this fuel tank is that it only weighs 5.7 kg. Using the tank specified above, the team is effectively able to satisfy requirement MO-1.4.

One of SWEEPs main objectives is to have a net positive effect on the debris-filled environment of low earth orbit. The team has ensured that this requirement will be met by placing a fuel tank on board the craft with enough hydrazine to continue the mission beyond the estimated lifespan, while also being able to deorbit itself into the ocean at the end of its lifetime.

4. Power

The Electrical Power Subsystem consists of 4 basic functions: Power Source, Energy Storage, Power Regulation and Control, and Power Distribution[42]. These 4 functions are all required to deliver the appropriate amount of power to each component of the spacecraft. The source for SWEEP is a set of Solar Panels which generate power while the spacecraft is in direct sunlight. The orbit chosen for the mission allows for the spacecraft to stay in sunlight for most of its orbit, but it will still pass behind the Earth into its Umbra on a few occasions throughout the lifetime of the mission. For these occasions, the instruments will be operating on reserve power via the Energy Storage system, which are a large set of batteries. Power Regulation and Control is performed by a board, the Power Control Unit (PCU), containing components which convert the DC power generated by the solar panel into an appropriate Voltage for the component that electricity is being delivered to. This board is connected to every component on the spacecraft via a set of insulated electrical cables which serve as the Distribution system. Each of these functions will be fulfilled by the components selected, which are described in their own sections below:

Power Source For power generation, the Roll Out Solar Array (ROSA) will be used. This choice was made due to the ROSA's low mass and high power per area. Given the table below describing specific mass and power values for roll-out solar arrays, one can work backwards to find mass and power per area. Configuration 2a was used in this case as this configuration matches closest with ROSA.

P_W/kW	r_{BM}/mm		m_W/kg		l/mm	w_W/mm	d_{env}/mm	
Conf2a-b	2a	2b	2a	2b	2a-b	2a-b	2a	2b
2.5	23	23	10.9	10.9	3,722	1,861	1,930	1,069
5	31	32	19.0	18.9	5,264	2,632	2,726	1,505
10	44	44	35.7	35.2	7,444	3,722	3,855	2,123
20	62	62	70.1	68.7	10,528	5,264	5,451	3,002
50	101	99	181.5	174.4	16,646	8,323	8,625	4,752
100	146	143	389.8	366.1	23,541	11,771	12,209	6,740
200	221	217	889.3	804.4	33,292	16,646	17,309	9,617
500	408	392	3,067.4	2,513.9	52,640	26,320	27,543	15,499

P_W/kW	m_{BM}/kg		m_{Bpv}/kg	m_{BS}/kg		k_{VEff}/kgm^{-3}		k_{Struc}	
Conf2a-b	2a	2b	2a-b	2a	2b	2a	2b	2a	2b
2.5	0.2	0.2	7.9	1.0	1.0	196.3	186.6	0.38	0.38
5	0.4	0.4	15.8	1.1	1.0	167.9	179.3	0.21	0.20
10	1.1	1.1	31.6	1.2	1.0	135.3	169.4	0.13	0.11
20	3.2	3.2	63.2	1.8	1.1	105.8	155.6	0.11	0.09
50	13.2	12.8	157.9	5.0	1.9	70.7	131.7	0.15	0.10
100	39.5	37.8	315.9	15.3	5.0	49.6	109.6	0.23	0.16
200	127.2	122.8	631.8	54.0	16.4	31.6	80.2	0.41	0.27
500	687.8	635.7	1,579.4	317.3	84.9	14.5	43.1	0.94	0.59

Fig. 20 Roll Out Solar Array Properties

First, let's determine the mass we can expect the solar array to have per area. We can take an example from the table to determine mass/area, then multiply that value by the area we select to determine an appropriate value for the mass of our panels.

$$Area = l * w_W$$

$$Area = 3.722 * 1.861 = 6.926642\ m^2$$

$$Mass = m_w + m_{BM} + m_{Bpv} + m_{BS}$$

$$Mass = 10.9 + 0.2 + 7.9 + 1.0 = 20\ kg$$

$$Mass\ per\ area = \frac{20}{6.926642} = 2.887\frac{kg}{m^2}$$

$$Power = P_w = 2.5\ kW$$

$$Power\ per\ area = \frac{Power}{Area}$$

$$Power\ per\ area = \frac{2.5}{6.9266} = 0.36093\frac{kW}{m^2}$$

Now we can assume that our ROSA is 6 meters long and 1 meter wide to calculate its area. This area is then multiplied by the Mass and Power per area to get the Mass and Power values for the ROSA.

$$ROSA\ Panel\ Area = 6 * 1 = 6\ m^2$$

$$ROSA\ Mass = Rosa\ Panel\ Area * Mass\ per\ area$$

$$ROSA\ Panel\ Mass = 6 * 2.8874 = 17.3244\ kg\ (X2)$$

$$ROSA\ Panel\ Power = ROSA\ Panel\ Area * Power\ per\ area$$

$$ROSA\ Panel\ Power = 6 * 0.360925 = 2.1655\ kW\ (X2)$$

A power output around 4.3311 kW provides ample power to fulfill EPS-1.1 and maintain a significant excess supply of power in the batteries of the spacecraft during eclipses. This remains true even at end-of-life of the spacecraft, assuming that the solar panels degrade by about 1% output per year (4.1188 kW after 5 years). Eclipses at an altitude of 900km can last as long as 42 minutes, which means the excess power supply of the batteries must have a capacity large enough to maintain operation of the payload and other components for at least that long:

$$Spacecraft\ Power\ Consumption * Maximum\ Eclipse\ Time = (3590.5W)(0.7hours) = 2513.4kWh$$

According to the paper, "Development of a Passively Deployed Solar Array," the deployment process for ROSA occurs using the sunlight that hits the rolled-up panel to thermally stretch the panel out. This process rolls out the panel at around 7.2m/hour. For our case, each 6m panel will take around 50 minutes to fully deploy at the beginning of the mission. The batteries chosen, fully charged at launch (4380 Whr -> 264 minutes of operation), gives the spacecraft an 164 minute margin to maintain critical component operation until the panels are fully deployed. Once the power source is operational and the electrical power supplied by the panels can be verified, the detection instrument can then be powered up.

Power Storage The Lithium-Ion Nickel-Cobalt-Aluminum-Oxide batteries provided by Eagle Picher [20] have a power capacity of 4380 Whr for a mass of 38.6 kg. This capacity is more than enough to provide power for all instruments throughout the longest possible Umbras even at end of life. Again, we can assume performance degradation around 1% per year to determine the capacity needed at end-of-life, which must be enough to last through a maximum-length Umbra, around 23 minutes.

Power Regulation and Control Each component has an interface which will accept only a specific Voltage and Current value from the power source. For each of those devices, a board will connect the solar panels to the batteries, and the batteries to every other component of the spacecraft. This board will need to consist of a large array of DC-DC power converters which deliver power to those devices at their expected values, as well as a device to measure the health and status of the EPS system, which communicates with the Comms system to provide command and telemetry capability for this information to the GSE, and finally several parts to protect the spacecraft against failures within the EPS and suppress transient bus voltages. Since spacecrafts are always custom-made for their mission, this means that a power regulation board is not available to purchase off-the-shelf like many other spacecraft components.

To find the mass needed for the Power Regulation system, compare the needs of the SWEEP spacecraft to those of RADARSAT, which used a Magellan Power Control Unit (PCU). [19]

For RADARSAT, their PCU had a mass of 27 kg and consumed 20W during operation, allowing the rest of the craft to function throughout the mission lifetime while also providing continuous telemetry for monitoring the health of the spacecraft bus and EPS. This PCU is also equipped with switch cards which regulate the excess power generated by the power source at beginning-of-life so that systems are not compromised by this excess generation. SWEEP's power needs are similar to those of RADARSAT, with peak operating power load around 3kW.

Power Distribution Each component on the spacecraft bus is connected to the PCU via an insulated cable. According to SMAD [42], a typical spacecraft will have about 4% of its EPS mass devoted to the cables. If we compare that to the mass of the remaining components of the system:

$$Mass = 38.6\ kg + 27.0\ kg + 34.648\ kg = 100.248\ kg$$

$$Mass_{cables} \approx 4.177\ kg$$

We can compare this to the result we find from determining the required thickness and length of each cable. The Power Bus voltage is 28±6 V(DC), so the minimum source voltage distributed will be around 22 V. The maximum voltage drop around 2% of that is industry standard:

$$V_{min} = 0.02 * (22V_{dc}) = 0.44V_{dc}$$

The wire resistance of any wire providing power needs to be lower than this maximum voltage drop divided by the current to that component. We can use this to determine the required thickness for each power distribution cable, and if we sum the mass of all those cables, we can determine the total mass for the EPS. [21] [22]

If the PCU is located near the center of the spacecraft, the longest cables will be from the PCU to the cameras and back to the PCU. That could be up to 5.0m in cases where the cable needs to ride along the wall of the interior of the spacecraft and around corners of other components. Therefore, a length of 5.0 m will be assumed for all cameras, since they are all roughly the same distance from the center of the spacecraft. The solar panels, star tracker, sun sensor, Earth Horizon Sensor, and LGA are also on the exterior of the craft, but all other components are inside and will have a total length <2.0 m. Lengths listed in the following table are calculated from the PCU to the component and back, to account for both cables run to each component. Approx. Mass is listed assuming that rubber insulation around each copper cable weighs approximately four times as much as the cable it is wrapped around, to be conservative.

Table 6 Power Cable Thickness by Component

Component	**Quantity**	**Current (A)**	**Resistance (Ohms)**	**Length (m)**	**Thickness (mm)**	**Approx. Mass (kg)**	**Total Mass (kg)**
Lasers	2	45	0.00978	3	0.912	0.0522	0.1044
Cameras	16	<0.60	0.73	5	0.405	0.0286	0.4578
Image Processing System	16	2	0.22	1	0.912	0.0174	0.2785
Solar Panels	2	75	0.005866	2	4.1	0.59125	1.1825
Star Tracker	2	0.125	3.52	3	0.143	0.002	0.004
Sun Sensor	2	0.012	36.67	3	0.08	0.00084	0.00168
SMU	1	12 (peak)	0.0367	2	1.15	0.1	0.1
Data Storage	1	0.455	0.967	2	0.227	0.0036	0.0036
Reactions Wheels	3	0.36	1.22	2	0.202	0.00285	0.00854
Magnetorquers	2	0.2	2.2	2	0.143	0.00143	0.00287
Magnetometer	2	0.03	14.67	2	0.08	0.0056	0.0112
Total Mass (kg)							2.0327

So, the total weight of all cable harnesses, including generous insulation, comes out to around 2.0327 kg. still somewhat lower than estimates for the power distribution subsystem of the EPS suggested in SMAD. It's conservative to assume that most of these cables (excluding only the lasers) will also need data cables from the component to the SMU. For this purpose, it is estimated that the data cables will have a mass around half of the power cables. That is equal to 1.01635kg for data cables, which connect the cameras to their respective image processing boards, those boards to the SMU, and the SMU to the antenna, as well as telemetry data for subsystem health and management to be communicated back to GSE, for a total of 3.04905kg for the Power Distribution Subsystem.

Here is the Block Diagram for the Electrical Power Subsystem, showing connections for Power, Data, and Mechanical interfaces between components on the spacecraft:

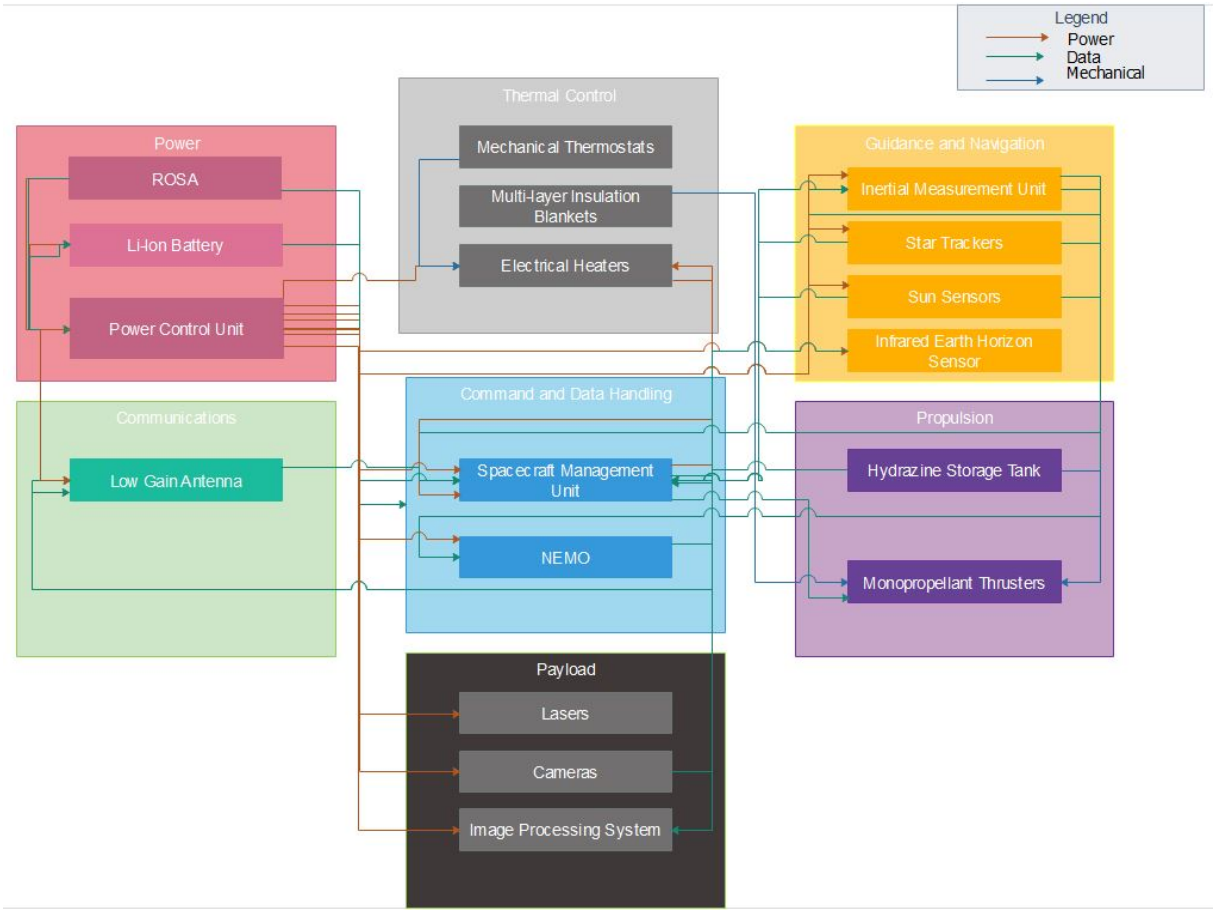

Fig. 21 Sweep EPS Block Diagram

5. Thermal

In order for the spacecraft to perform optimally, an operating temperature should be maintained. This operating temperature will depend on external temperatures, individual instrument tolerances, as well as methods used to maintain or expel heat. The external temperature found in Low Earth Orbit falls in the range of -65 to 125 ºC.[23] From various sources the black body temperature of an object in Low Earth Orbit is around 255K (-18.5 ºC).[24] This essentially would be the temperature of the craft without the heat generated from its various instruments. This "stable" temperature fits within the operating range of all of our instruments except the battery, but of course will increase due to the use of our various components. The thermal tolerances of each component on the spacecraft are displayed in the table below.

Table 7 Thermal Tolerances

Component	Tolerance
Reaction Wheel	-5 to 50ºC (Mineral Oil) -20 to 70ºC (Synthetic Oil)
Star Tracker	-40 to 30ºC
IMU	-54 to 71ºC
Sun Sensor	-50 to 71ºC
Rosa	-60 to 60ºC
Battery	10 to 30ºC

To get a better sense of the thermal control needed on the SWEEP satellite calculations can be made to determine heat absorbed due to the instruments as well as sun. Another calculation of heat loss due to potential colder temperatures in LEO can also be made. This will determine the rise in temperature of the spacecraft for a given time period.

First heat absorption is calculated. This is done by converting the heat generated by a particular component (in Watts) to temperature increase per time (ºC/s). A sample calculation of converting the laser instrument is provided below.[25]

Total Power = 3.112 kW = 3112 W
Efficiency = 0.25
*Leftover Power = P = 3112 - 3112*0.25 = 2334 W*
Running Time = t = 1 s
Mass = m = 500000 g
Specific Heat Capacity = C = 0.92 j/g ºC

$$\Delta T_{absorb} = \frac{Pt/m}{C}$$

$$\Delta T_{absorb} = \frac{(2334 * 1)/500000}{0.92}$$

$$\Delta T_{absorb} = 0.005074 C/s$$

This calculation is expanded upon to include heat generation from all on board instruments. The table of these calculated values is below.

Table 8 Thermal Absorption

Component	Temperature Increase (ºC/s)
Reaction Wheel	0.000782609
Star Tracker	1.413*10^(-5)
IMU	2.61*10^(-5)
Sun Sensor	0.000217
Laser	0.005074
ROSA	0.009415
Solar Radiation	0.008922
Magnetorquers	0.008696
Horizon Sensor	1.43*10^(-5)
Power Control Unit	0.00013
Total	**0.033292**

Next the heat loss is calculated. This is calculated using the net radiation loss rate equation. In this case an extreme operating temperature of -20 ºC was used and an ideal craft temperature of 10 ºC was used. The equation and calculation are below.[26]

Emissivity = e = 0.64
*Stefan-Boltzmann Constant = σ = 5.6703*10-8 W/m2K4*
*Object Area = A = 3m *.5m*
Object Surface Temp = Th = 10 ºC = 283.15 K
External Temp = TC = -20 ºC = 255.15 K

$$Q = e\sigma A(T_h^4 - T_c^4)$$
$$Q = 0.64 * (5.6703 * 10^(-8)) * (3 * 0.5) * (283.15^4 - 255.15^4)$$
$$Q = 119.1933 \frac{W}{m^2}$$

This gives the value for only one surface of the craft, so the calculation must be repeated for each surface. The same temperature to wattage equation used for heat absorption is used again for heat loss producing the value below. This value can then be subtracted from heat absorption to find total change in temperature.

$$\Delta T_{loss} = 0.001576^\circ C/s$$
$$\Delta T_{loss} = \Delta T_{heat} - \Delta T_{loss}$$
$$\Delta T_{loss} = 0.033292 - 0.001576$$
$$\Delta T_{loss} = 0.031716^\circ C/s$$

Taking into account the temperature range of Low Earth Orbit, solar radiation, and heat generation from components gives a net increase in the temperature of the spacecraft. To counteract this a method to dump heat from the spacecraft is needed. One such method is the use of a radiator which uses an exposed surface area with high emissivity to expel heat. The radiator would be part of a louver system which would open, exposing the radiator when the spacecraft is getting too hot and close when the spacecraft is getting to cold. The radiator material of choice is a graphite-fiber-carbon matrix composite. This radiator has both high emissivity at 0.9 and low mass, which is ideal in our case. It has a specific mass of 1.45 kg/m^2, which works out to 9.425 kg for our radiator.[27] To go along with the radiator, reflective sheeting will be lined along the outside of the craft to reduce the effect solar radiation absorption. The sheeting chosen is a 1 millimeter ITO coated silver FEP from Sheldahl. Coming in at 54 g/m^2 the total sheet weight would be 351 g, or 0.351 kg.[28]

6. Command and Data Handling

The main priorities of this subsystem is as follows:

1) Monitor power and thermal properties of major sub-systems
2) Process and select relevant data from camera output
3) Transmit and monitor spacecraft status
    - Outputs of attitude sensors
    - Propulsion usage

Both the telemetry data of the spacecraft as well as the data of debris will be analyzed on ground systems. Beyond the processing memory required, the actual onboard data storage of debris detection is very minimal and even with basic instrumentation. The main priority then becomes processing the images from the array of cameras.

To capture the light from debris passing through the disk, the payload's cameras require a very high frame rate of at least 5 million images a second. Each of the 16 cameras have 6000x3000 (18 Megapixels) pixels, which collects about $1.07 * 10^{13}$ Bytes/second. This is a near impossible task to process all the data in the given amount of time. Possible methods to mitigate this issue are described within the conclusion of the paper. The following section describes an idealized image processing system to show how the calculations and the hardware selection procedure would be completed.

One 20MP image will take up approx. 7MB of storage space, for debris detections on the interior of the disk, each scattering event may be seen by three cameras independently on each laser-disk projected by the spacecraft. This gives us about (7MB* 6 images)=40MB of data to communicate per debris detection so that the raw images can be analyzed in detail to confirm the position and trajectory measurements taken by the payload.

In order to process each image enough to determine whether it is worth saving and communicating back to the ground, all that is necessary is a simple thresholding operation. This calculation compares the intensity of each pixel to a specifically chosen threshold. This threshold value needs to be decided carefully in order to effectively discard noise without losing valuable information. Since the laser's wavelength is well beyond the spectrum produced by the Sun and most other satellites do not communicate at this wavelength, it is relatively safe to assume that noise will be low and thus that the chosen threshold can be low, perhaps 10/255 pixel intensity, though experimental testing to verify a more specific number will be necessary.

Each image is thresholded, becoming a monochromatic black/white image. If this image consists of all black, indicating that the camera detected only noise and discarded the unnecessary light points, the image is discarded. If there are white pixels in the thresholded image, this indicates a scattering event which was captured by the camera. This image and its corresponding threshold mask are stored for communication to the ground, along with the precise timestamp and telemetry data indicating which camera took the image. This data will be sent to GSE where the brightest pixels of the image can be used to determine the relative position of the scattering event. Another image should be detected on the other disk to confirm that this data was not noise, and together, the relative position of the scattering event and the time delay between events can be used on the ground to effectively determine the orbital characteristics of the passing piece of debris. This information can then be communicated to the Johnson Space Center Orbital Debris Tracking Center, where it can be used in the future to mitigate risks to U.S. spacecraft.

Image processing required for each camera can be calculated using the following equation. Assume (conservatively) that each pixel requires approx. 4 floating point operations (flops) to process using the basic thresholding operation:

$$Processing\ Power = (4\ flops/pixel) * (20 * 10^6\ pixels/camera) * (18\ frames/sec)$$

$$Processing\ Power = 1.44\ teraFLOPs/camera$$

Our sensor stores images as an m*n matrix, as it gives the intensity of light detected at that pixel, and not as a 3 channel RGB image like most cameras do. This reduces the number of operations required for each image by a factor of 3, and this factor is included in the equation above.

This calculation also assumes unoptimized calculations done on a CPU. With an optimized GPU setup as recently demonstrated at Nvidia's GTC, we can accomplish the same task with one Jetson Nano board for each camera. These boards are tiny, 100mm*80mm*29mm, and are designed to connect to cameras via a 12 lane 1.5 Gbps connection which can support 4K resolution at up to 60 frames per second, or higher resolutions at lower frame rates, in our case. Each consumes 5-10W. If we include one of these boards per camera, that raises our power budget by 160W. Each board has a mass around 0.10 kg. They have an image processing capability of around 2.5TFLOPS, just larger than our requirements per camera, which make these boards convenient to power each camera.[38]

Onboard data storage should be approximately 150 MB, as it should conservatively hold 3 debris detections of 120 MB total and any relevant spacecraft health and status data, which would be 30 MB.

Data Storage:

NEMO:[37]

1) Provides 512 Gbit data storage (flash memory) with replay capability.
2) 6.6 kg mass, volume 365mm*135mm*235.
3) Data rate: 120Mb/s input, 310Mb/s
4) Only stores images which, after processing, have been marked as valuable data and are saved to later be communicated to the ground. Other images are stored on 16GB SD cards on the Nvidia Jetson Image Processing boards until they are processed and deleted.

7. Communications System

In order to determine the appropriate data rates required for the communication system, both the size of the data as well as the visibility of the ground station must be known. This visibility window is illustrated by the shaded region below, assuming there is a 180 degree visibility.

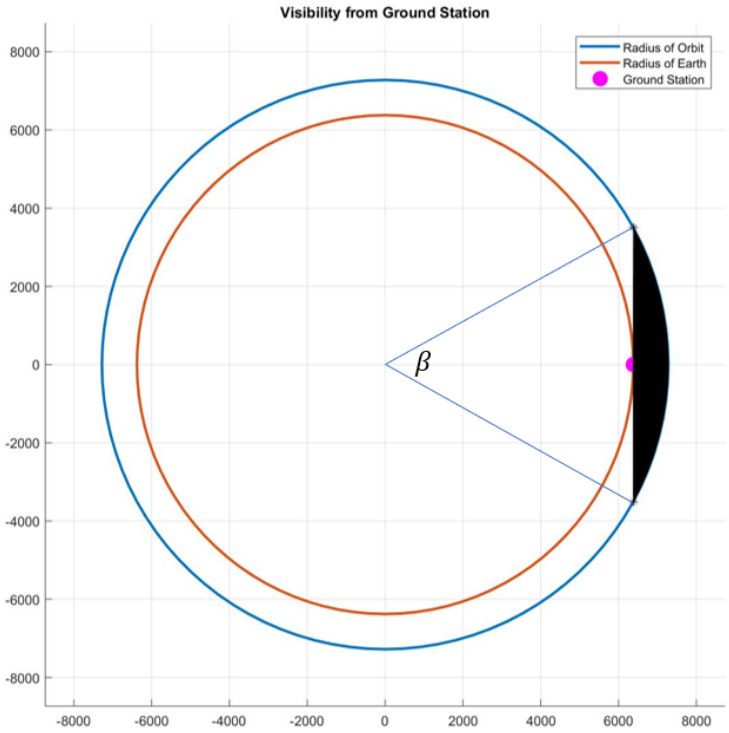

Fig. 22 Visibility From Ground Station

To find the visibility time, we can simply solve for the angle and compare it to the entire orbit.

$$\beta = 2 * tan^{-1}\left(\frac{\sqrt{R^2 - r^2}}{r}\right)$$

$$Percentage\ of\ Orbit\ Visible\ from\ Ground\ Station = \frac{\beta}{360} * 100$$

Plugging in the radius of the earth for r and the radius of the orbit for R, the following can be shown.

$$\beta = 2 * tan^{-1}\left(\frac{\sqrt{(6378 + 900)^2 - 6378^2}}{6378}\right)$$

$$Percentage\ of\ Orbit\ Visible\ from\ Ground\ Station = 16\%$$

It is known that total time of our orbit is 103 minutes, and can therefore be said that the total time where the spacecraft is visible from the ground station is 16.5 minutes each orbit. This is assuming a perfectly circular orbit and 180 degree visibility of the ground station.

It has been estimated that there will only be a debris detection every 47 days, and the orbit is 103 minutes. This clearly shows that we should have very little actual data to transit for each orbit beyond regular spacecraft diagnostics.

The Low Gain Antennas have been selected from the FireSat communications system[39], and the details have been laid out below. The system chosen has a downlink data rate of 90 kbps, where 40 kbps has been allocated for spacecraft health and status and the remaining 50 kpbs reserved for debris detection data. This system uses UHF as the frequency is listed as 2.3 GHz.

Downlink Budget					
Parameter	Value	Units	Parameter	Value	Units
Frequency	2.3	GHz	Link Propagation Losses	-163.7	dB
Wavelength	0.130435	m	Free-Space Loss	-159.7	dB
Range	1000	km	Rain & Clouds	-4	dB
RX Background Noise	10	deg-K	RX Gain	26.5	dB
TX PA Output Power	8	W	Antenna Gain	28	dB
RX Antenna Diameter	0.5	m	Surface Roughness Loss	-0.5	dB
RX Antenna Efficiency	55	%	Waveguide Loss	-1	dB
RX Antenna Beamwidth	22	degrees	Received Isotropic Power	-133.2	dB(W)
RX Aperture Efficiency	0.55	%	Noise Denisty	-199.6	dB(W/Hz)
RX Waveguide Temp	300	degrees-K	Background Noise	85.6	deg-K
RX Receiver Noise Figure	5	deg-K	RX Receiver Noise	709.6	deg-K
Required C/No	55	dB(Hz)	Total RX Noise	795.2	deg-K
EIRP	4	dB(W)	RX G/T	-2.5	dB(/deg-K)
TX PA Output Power	5	dB(W)	C/No	66.4	dB(Hz)
TX Guide Loss	-1	dB	Required C/No	55	dB(Hz)
TX Antenna Gain	0	dB	Excess Margin	11.4	dB

Fig. 23 Downlink Budget

Uplink Budget					
Parameter	Value	Units	Parameter	Value	Units
Frequency	2.1	GHz	Link Propagation Losses	-170.9	dB
Wavelength	0.1428571	m	Free-Space Loss	-158.9	dB
Range	1000	km	Rain & Clouds	-12	dB
RX Background Noise	300	deg-K	RX Gain	-1.5	dB
TX PA Output Power	14	W	Antenna Gain	0	dB
RX Antenna Diameter	0.5	m	Surface Roughness Loss	-0.5	dB
RX Antenna Efficiency	55	%	Waveguide Loss	-1	dB
RX Antenna Beamwidth	24.1	degrees	Received Isotropic Power	-147.2	dB(W)
RX Aperture Efficiency	55	%	Noise Denisty	-199.2	dB(W/Hz)
RX Waveguide Temp	400	degrees-K	Background Noise	341.9	deg-K
RX Receiver Noise Figure	4	deg-K	RX Receiver Noise	521	deg-K
Required C/No	45.5	dB(Hz)	Total RX Noise	862.9	deg-K
EIRP	25.2	dB(W)	RX G/T	-30.9	dB(/deg-K)
TX PA Output Power	8	dB(W)	C/No	52.1	dB(Hz)
TX Waveguide Loss	-1	dB	Required C/No	45.5	dB(Hz)
TX Antenna Gain	18.2	dB	Excess Margin	6.6	dB

Fig. 24 Uplink Budget

The subsystem is sized for 10 kbps uplink data rate, which can be used for the following:

1) Correcting attitude
2) Battery Reconditioning
3) Thruster Firing
4) Switching heaters of various subsystems

Using these values listed above, the transmission time for one debris detection can be calculated as shown below.

$$Time\ of\ Transmission = \left(\frac{Size\ of\ Data}{Transmission\ Rate}\right)$$

*Size of Data for one Debris Detection = 40 MB = 320*10e6 bits*
*Transmission Rate = 50*10e3 bits/second*

$$Time\ of\ Transmission = \left(\frac{320 * 10^6 bits}{50 * 10^3 bits/sec}\right) = 6400\ seconds = 106.67\ minutes$$

This long duration of data transfer is completely acceptable as only one debris is expected to be gathered every 47 days. Performing a similar calculation, the amount of data transmitted for each orbit can be shown below.

$$Amount\ of\ Data\ Transmitted = Time * Transmission\ Rate$$

$$Amount\ of\ Data\ Transmitted = \left(16min * 60\frac{sec}{min}\right) * \left(90 * 10^3 \frac{bits}{sec}\right)$$

$$Amount\ of\ Data\ Transmitted = 864 * 10^5 bits = 10.8MB$$

The relevant power and mass for the entire communication system can be shown below.

Description	Power (W)	Mass (kg)
Command Receiver (2)	12	5.25
TM Trasmitter (2)	7	3.88
TM SSPA (2)	14	2.69
Total Communication System	33	11.82

The data will also be sent to the Johnson Space Center, as they already have a ground based debris detection center and this will contribute to their progress.[40]

8. Guidance, Navigation and Control

For attitude control and stabilization we have a number of options that could satisfy our requirements. The use of momentum wheels, CMG's, reaction wheels, or even gravity gradients with momentum wheel bias, are all valid means of attitude control, each with their own benefits and drawbacks. A pitch-momentum wheel and thruster combination would be able to keep SWEEP controlled about 3 axes, but would require frequent pulsing from the thrusters. A gravity gradient would be able to keep SWEEP constantly facing nadir for the entire duration of the mission, however its level of accuracy is reported from SMAD to be only practical for missions that require less than 1 degree of accuracy from the attitude determination system. This is nowhere near the 360 arcseconds of accuracy declared by requirement GNC-3.1. A three reaction wheel system was ultimately chosen due to its high pointing accuracy about each independent axis, low power demand, and relative simplicity.[29] Reaction wheels work by storing angular momentum, and it was found that approximately every 100 kg requires 1 Nms.[30] Based off of this approximation, SWEEP would require a minimum of three 5 Nms reaction wheels.

To account for disturbances caused by gravitational perturbations, drag, solar panel gimbals, solar pressure torques, jitter, fluid sloshing, and dynamic flexing of the vehicle chassis; the team has decided to go with four RW8 reactions wheels from Blue Canyon Tech. They provide up to 8 Nms each with low mass and power usage.[31] A fourth reaction wheel will also be implemented as a contingency for an unexpected failure of any of the three main wheels.

According to SMAD, it is typical of Earth pointing satellites to have a 3 axis stabilized setup scheme consisting of three star trackers, four sun sensors, two infrared Earth horizon sensors, one magnetometer, and three magnetorquers (if using three reaction wheels). This attitude determination suite will be crucial to the accurate operation of the laser disc system. Since SWEEP's primary laser-disc debris detection payload will require us to constantly know our position in our orbit and relative to the earth; we will need targeting instruments that have the ability of satisfying that requirement. SWEEP will need to have the ability to fine tune its orientation and counteract all the disturbances listed in the analysis

below. More importantly however, SWEEP will need to constantly be aware of its orientation in 3 axes at all times, per requirement GNC - 3.1. As a result the team has selected the T1 Star Tracker to achieve this level of accuracy. The T1 is equipped with an optical head that has a 1.5 arc-second accuracy (.0004 degrees) and an advanced photo system resolution of 1024 x 1024 while only requiring 3.25 Watts each. Four of these units will be placed on SWEEP, with one being used for redundancy.[33]

The inertial measurement unit for SWEEP was chosen by examining heritage components from past GEO and LEO satellite missions. The IMU that was selected was Northrop Grumman's LN-200S. This selection was made due to the LN-200S's highly reliable attitude reference, as well as past usage on heritage missions in low Earth orbit.[34]

The sun sensor that was chosen for SWEEP was Bradford Space's Fine Sun Sensor. This sensor was chosen due to its specific low earth orbit qualifications. It is capable of enduring large temperature swings (-50 to +85 C), as well as intense radiation exposure of 100 kRad. It is capable of an accuracy of less than .3 degrees for 2 -axis knowledge of the suns position, which should be more than enough for SWEEP's large solar panels. Along with this, its unobstructed field of view is 138 x 138 degrees and its overall power consumption is .25 Watts. Per SMAD recommendations, SWEEP will be equipped with four actively operating sun sensors, and a fifth, for redundancy. [35]

While the star trackers will be the primary means of attitude determination, an earth (nadir) pointing satellite still needs to have an understanding of where the earth's horizon is at. That is why the group has selected the IRES-C Infrared Earth Sensor from Selex Galileo. With an accuracy of .6 degrees, and a maximum power consumption of 3.3 watts the IRES- C will enable SWEEP to constantly know its pitch and roll with respect to its flight path. It will be outfitted with two of these units.

Desaturation Method Determination In order to determine whether thrusters or magnetic torquers should be used when desaturating, various calculations were made to track the feasibility of both. Almost every calculation made throughout this investigation used the worst case scenario values. For example, the value of magnetic field that was used for determining the magnetometer, was the lowest intensity that SWEEP would experience throughout its lifetime. Conversely, when calculating the electromagnetic induced disturbance torque, the highest value was used.

The first values that needed to be produced in this analysis were the moments of inertia about the different axes. This was done to determine what the worst case scenario was for pitch, roll and yaw. In table 19 and 20, one can observe that two different inertial orientations were considered. The Parallel Configuration occurs when the solar panels are parallel with the flight path of SWEEP. This configuration is achieved when the sun is directly overhead/zenith/anti-radial of SWEEP. The other configuration is when the solar panels are oriented perpendicular to SWEEP's prograde flight direction. The results of this calculation show that for both configurations, the pitch axis has a moment of inertia of 361.61 (kg. m2). This is a pretty manageable value. This axis must be under the greatest amount of control since the vehicle will need to have a continuous slew rate of .058 degrees per second.

Now that the team was aware of the inertial properties of SWEEP, disturbance torques could be explored. Using SMAD, the team was able to calculate every natural and spacecraft-induced torque disturbance with a factor of safety higher than 1.2. These calculations represent the worst case torque that the spacecraft would experience. This is what SWEEP would need to overcome during normal flight operations. This value includes solar torque, gravitational torque, atmospheric torque and torques caused by Earths magnetic field. The value determined here was a driving factor used in determining the capability of both the magentorquer and the thrusters. These calculations can be seen in Table 21.

The next set of calculations were made to determine the size of the magnetic torquer that would be needed in order to desaturate SWEEP's reaction wheels. The slew torque and momentum storage required were first found. From this, the required size of magnetorquer in (A/m 2) was calculated. The value itself can be found in Table 22. Table 23 goes on to determine what kindof thruster SWEEP would need to have in order to acomplish the same job. The force, and total pulse time were determined. From these, the mass of fuel in kilograms that would need to be stored onboard, was dsicovered.

Over precisely one quarter of the spacecraft's orbit, the reaction wheels will reach saturation. If thrusters were used to desaturate, this would mean that they would have to fire approximately, 55.9 times a day since SWEEP's orbit last roughly 103 minutes. Instead, to battle desaturation, three magnetorquers and one magnetometer will be used. By passing through the Earth's magnetic field, all three of the EM coils will be able to generate a 40(A/m 2) current which will easily be able to desaturate the wheels over time, and create the .058 degree per second slew rate that SWEEP will need in order to constantly be in a prograde facing direction. In the analysis conducted below, it can be seen that if the team had decided to go with desaturation thrusters, SWEEP would've had to fire its thrusters for approximately 69.9 hours over the course over an anticipated 5 year mission lifetime. This works out to be 719.4 kg of hydrazine; an

amount that is entirely impractical to store onboard the spacecraft. It is for these reasons that the most logical path forward would be to use three 40 (A/m 2) magnetorquers, which only require 1 W every time they are fired. [32]

The primary conclusion of this investigation is that it would be far simpler to use magnetic torquers in tandem with a magnetometer. The team has made the decision of retaining the six original thrusters on the vehicle. Only now, they will no longer be used for desaturation. For the final design of SWEEP, the team determined that SWEEP would need to keep the translational thrusters for deorbiting and station keeping. The two rotational thrusters could then instead be used for an emergency high rate roll maneuver or emergency desaturation if the need were to ever arise throughout the lifetime of the mission. The elimination of desaturation fuel would result in enormous mass savings, as well as reduce the complexity of the design. In order to permit the use of magnetorquers, SWEEP would need to be outfitted with an additional instrument. This lead to the selection of the MAG-3 Three Axis Satellite Magnetometer. This instrument was especially designed for low Earth orbit satellites. SMAD indicates that if your spacecraft is orbiting under 6000km, the magnetometer should be capable of one degree of accuracy. The magnetometer that was selected will permit an accuracy of .75 percent.

Fig. 25 Inertia Coordinate Frames

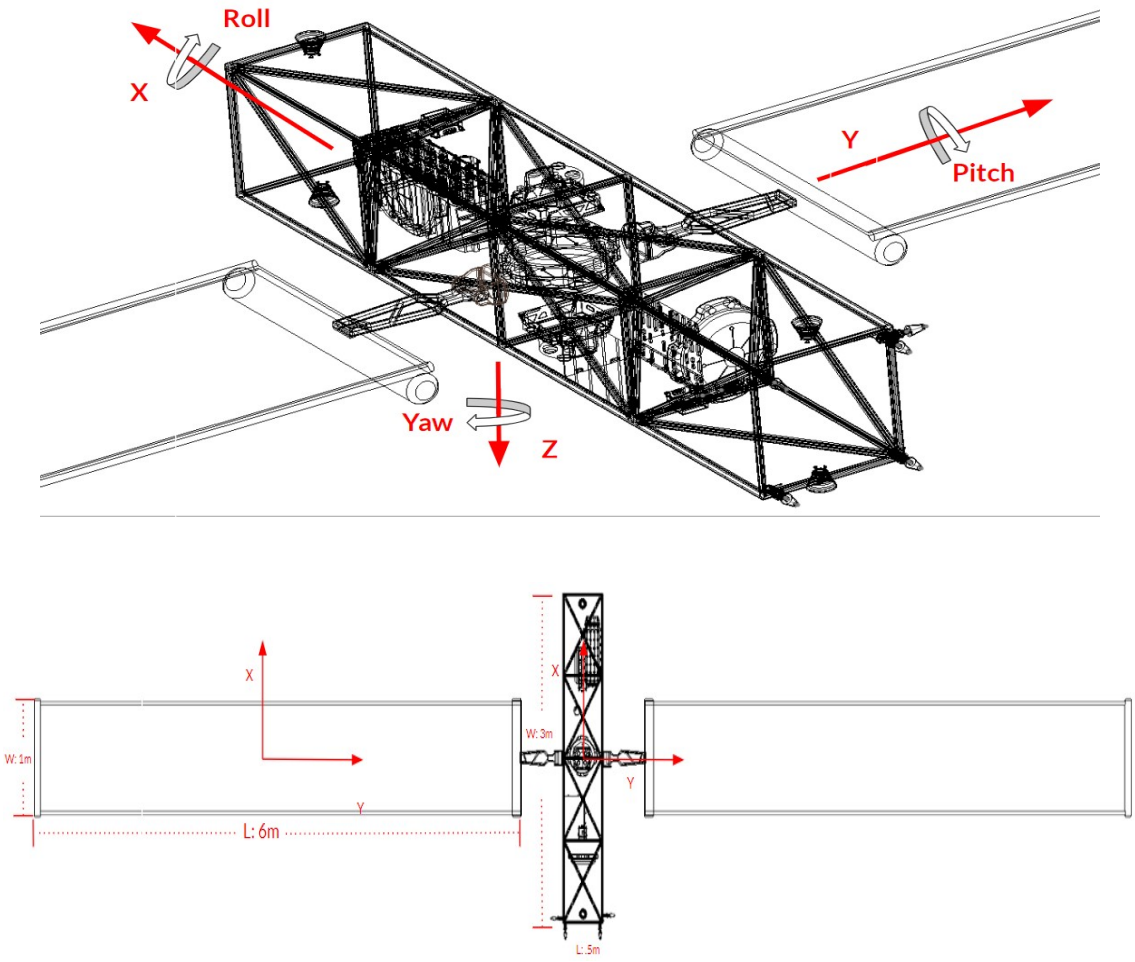

Table 9 Moment of Inertia - Parallel Configuration

Ix (Roll)			
Solar Panels (x2)		Chassis	
l (m)	6	l (m)	0.5
w (m)	0.05	w (m)	0.5
m (kg)	17.32	m (kg)	465.36
Ix (kg m^2)	103.93	Ix (kg m^2)	19.39
Ix (kg m^2)	123.32		
Iy (pitch)			
Solar Panels (x2)		Chassis	
w (m)	1	w (m)	3
h (m)	0.05	h (m)	0.5
m (kg)	17.32	m (kg)	465.36
Ix (kg m^2)	2.89	Ix (kg m^2)	358.72
Iy (kg m^2)	361.61		
Iz (Yaw)			
Solar Panels (x2)		Chassis	
l (m)	6	l (m)	0.5
w (m)	1	w (m)	3
m (kg)	17.32	m (kg)	465.36
Ix (kg m^2)	106.81	Ix (kg m^2)	358.72
Iz (kg m^2)	465.52		
Moment of Inertia (kg m^2)	**950.45**		

Table 10 Moment of Inertial - Perpendicular Configuration

Ix (Roll)			
Solar Panels (x2)		Chassis	
l (m)	6	l (m)	0.5
w (m)	1	w (m)	0.5
m (kg)	17.32	m (kg)	465.36
Ix (kg m^2)	106.81	Ix (kg m^2)	19.39
Ix (kg m^2)	126.2		
Iy (pitch)			
Solar Panels (x2)		Chassis	
w (m)	0.05	w (m)	3
h (m)	1	h (m)	0.5
m (kg)	17.32	m (kg)	465.36
Ix (kg m^2)	2.89	Ix (kg m^2)	358.72
Iy (kg m^2)	361.61		
Iz (Yaw)			
Solar Panels (x2)		Chassis	
l (m)	6	l (m)	3
w (m)	0.05	w (m)	0.05
m (kg)	17.32	m (kg)	465.36
Ix (kg m^2)	103.93	Ix (kg m^2)	349.12
Iz (kg m^2)	453.04		
Moment of Inertia (kg m^2)	**940.85**		

Table 11 Worst Case Disturbance Torque

Solar Radiation Pressure	
Solar Constant Fs (W/m^2)	1367
Speed of Light c (m/s)	3.00E+08
Area As (m^2)	13.5
Reflectance Factor q	0.6
Incident angle of Light I (deg)	0
Solar Force F (N)	5.64E-03
Cps-cg (m)	0.1
Solar Torque Tsp (Nm)	**5.64E-04**
Gravity Gradient Disturbance	
Ix	123.32
Iy	361.61
Iz	465.52
Orbital Parameter mu (m^3/s^2)	3.99E+14
Orbital Altitude (m)	7278000
Maximum Deviation of Z (rad)	1.75E-03
Gravitational Torque Tg (Nm)	**1.85E-06**
Magnetic Field Disturbances	
Residual Dipole D (Am^2)	1
Magnetic Moment M (tesla*m^3)	7.96E+15
Radius from the Dipol R(m)	7278000
Earth's Magnetic Field B (tesla)	4.13E-05
Torque Atmospheric (Nm)	**4.13E-05**
Aerodynamic Disturbances	
Density of Air at (900km)	1.18E-15
Coefficient of Drag	2
Area (m^2)	13.5
Orbital Velocity (m/s)	7,400.53
Force From Drag F (N)	8.72E-07
Cpa-cd	0.3
Torque Atmospheric (Nm)	**2.62E-07**
Total Disturbance Torque (Nm)	**7.29E-04**

Table 12 Reaction Wheel Sizing

Slew Torque	
Distance of Max Slew (rad)	3.14
Time allowable time (s) (T/2)	3,089.58
Inertia of largest Axis (Iz)	465.52
Slew Torque Required T (Nm)	**6.13E-04**
Momentum Storage in RW	
Sinusoidal average (Nms)	0.707
Total Disturbance Torque	7.29E-04
Orbital Period (s)	6179.15797
Momentum Storage Required (Nms)	**7.96E-01**
Magnetorquer Needed (A*m^2)	
Worst Case Magnetic Field B (tesla)	2.06E-05
Total Disturbance Torque	7.29E-04
Magnetorquer Needed D (Am^2)	35.3
Magnetorquer Length (m)	0.208
Total Magnetorquer Mass (kg)	**4.576**
Total Power Needed (W)	**4**

Table 13 Thruster Sizing

Thruster Force Level	
Total Disturbance Torque (Nm)	7.29E-04
Moment Arm L (m)	0.25
Force Needed (N)	**2.92E-03**
Sizing Force Level to Slew Rate (deg/s)	
Change in Angle (deg)	0.6
Time Allotted for Maneuver (s)	10
Rate (deg/s)	0.06
Time Spent Accelerating (%)	0.05
Time Spent Accelerating (s)	0.5
Rate of Acceleration (rad/sec)	2.09E-03
Amount of Thrust Needed (N)	**3.9**
Sizing for Momentum Dumping	
Number of Axes	3
Start and Stop	2
Times per Day	55.92
Days	365
Years	5
Total Number of Pulses	612349.5
Total Time Spent Pulsing (s)	612349.5
Total Time Spent Pulsing (hr)	**69.9**
Equivalent Velocity Veq	2,255.53
Specific Impulse Isp	230
Thrust	2.65
Time of Burn tb	612349.5
Amount of Fuel Needed (kg)	**719.46**

External Torque Disturbances Equations

Gravity Gradient
$Max\ Gravity\ Torque = T_g$
$Earth's\ Gravity\ Constant = \mu$
$Orbital\ Radius = R$
$Maximum\ Deviation\ of\ Z\ axis = \theta$
$Moments\ of\ Inertia = I_y, I_z$

$$T_g = \frac{3\mu}{2R^3}|I_z - I_y|sin(2\theta)$$

Solar Radiation
$Solar\ Radiation\ Pressure = T_{sp}$
$Solar\ Constant = F_s$
$Speed\ of\ Light = c$
$Surface\ Area = A_s$
$Center\ Solar\ Pressure\ Location = c_{ps}$
$Center\ of\ Gravity = c_g$

$Reflecatance\ Factor = q$
$Angle\ of\ Incidence\ of\ the\ Sun = l$

$$T_sp = F(c_{ps} - c_g)$$

$$Where\ F = \frac{F_s}{c} A_s(1+q)cos(l)$$

Magnetic Field
$Magnetic\ Torque = T_m$
$Residual\ Dipole\ of\ Vehicle = D$
$Magnetic\ Moment\ of\ Earth = M$
$Radius\ from\ Earth\ Center\ to\ Craft = R$

$$T_m = DB$$

$$Where\ B = \frac{2M}{R^4}$$

Aerodynamic
$Aerodynamic\ Density = T_a$
$Atmoshperic\ Density = \rho$
$Drag\ Coefficient = C_d$
$Surface\ Area = A$
$Spacecraft\ Velocity = V$
$Center\ of\ Aerodynamic\ Pressure = c_{pa}$
$Center\ of\ Gravity = c_g$

$$T_a = F(c_{pa} - c_g)$$

$$Where\ F = 0.5[\rho C_d A V^2]$$

Momentum Storage from Reaction Wheel
$WheelMomentum = h$
$Worse\ Case\ Disturbance\ Torque = T_D$

$$h = (T_D)\frac{Orbital\ Period}{4}(0.707)$$

Torque from Magnetic Torquers
$Magnetic\ Dipole = D$
$Worst\ Case\ Disturbance\ Torque = T_D$
$Earth's\ Magnetic\ Field = B$

$$D = \frac{T}{B}$$

9. Structures and Mechanisms

Shape The Primary structure of the vehicle is 3 meters long and .5 meters in width and height. The main reason this length was selected was to increase the distance between the aperture of the cameras and the laser sheet. The farther the cameras are away from the scattering event, the easier it is for the camera's field of view to envelope every section of the laser plane. When the team was in the early design phase for the chassis of SWEEP, a boom/extension mechanism was being considered for use. The idea was to attach the mirror onto this mechanism and have it extend out about 10 meters from the main structure. Doing this would allow for much more manageable camera envelopment of the disc, however it lead to much larger concerns. Since the SWEEP spacecraft is an Earth pointing satellite, that means it must constantly being slewing. With this constant motion it is reasonable to expect that the extension mechanism will begin to flex back and forth at its resonant frequency. This would yield a large amount pointing and alignment uncertainty in the laser-disc mirror setup. It would also make it far more challenging for the team to achieve the attitude and determination requirement GNC-3.1. The larger the extension, the worse this effect would be. As a result the team had to find a happy middle ground; a design that would yield a large value of radius r, (distance from the aperture to the mirror) while

reducing the amount of vibrational modes and moments of inertia. It was decided that the team would attempt to make the structure as rigid as possible.

One of the early rigid structures consisted of a three meter long hexagonal prism, this can be seen in the appendix. This honeycomb structure is not unique. It has been used on many spacecraft in the past like the HEAO-B and the FLTSATCOM. It is typically appealing due to the strength and rigidity it gives the chassis. While this design was visually appealing to the team, a much more grounded approach was chosen due to its simplicity and familiarity. The FEA analysis showed that designing the frame of the vehicle using a triangular truss technique would be the best route to go. This method is backed by many heritage missions as well as SMAD.

> *"We use cylindrical and conical shell structures and trusses for primary structure, commonly building them out of aluminum and magnesium with titanium for end fittings." (Space Mission Analysis and Design Pg. 335)*

Space Allocation One major difficulty of sizing the chassis of SWEEP was how long to make the vehicle. The team was aware that SWEEP would need larger solar panels in order to generate the necessary power. A reasonable length of the chassis that was proposed, was 3 meters. The team decided to start with this length and investigate whether or not it would be a reasonable dimension. If the cameras were mounted on the end of the vehicle, that would mean that the value of r would be 3m and the camera scheme would be able to get decent coverage of all points on the disc. However, this design choice brought another set of issues into the spotlight. Since the cameras must have 360 degree coverage of the disc, that means they must be mounted on every side panel on the SWEEP craft. This meant that no matter where the solar panels were placed, or what shape they were, we were going to end up covering some portion of the cameras view. A this point the team determined that it if the panels were going to block any section at all, that it would be beneficial to make the solar panels long and slender instead of short and wide. This would allow the team to minimize the percentage of blocked area on the region on the disc that would be capable of detecting debris down to 1mm in size.

Eventually it was determined that it was impractical to allow the solar panels to cover such a significant portion of the view. Instead, the team decided to move the cameras from the forward and aft ends of the vehicle, to the center of it. This is the current configuration used in the final design. This would yield a radius of r=1.5m. This still enables the cameras to cover a large portion of the disc, only now there would have to be additional cameras. This turned out to be a very manageable issue since the cameras required relatively little power and took up little space.

Another large effort that went into sizing the chassis was the space allocation analysis. The team wanted to verify that all the components that were being selected (except the solar panels) were capable of being housed within the primary structure of SWEEP. In the visualizations shown throughout the document (appendix sections C through G) one can see that many instruments that had publicly available dimensions, were modeled in CAD and placed within the primary structure to verify if the chassis was sized appropriately.

Material The choice of material for the primary load bearing structure of the SWEEP craft was an Aluminum Lithium Alloy. Specifically, Aluminum 2099. This alloy is used on many past missions, and is recognized as having many attractive attributes that make it an excellent choice for the main chassis of the vehicle. It has been used on the aerostructures of the A380, A350 as well as the B777X. Other aluminum lithium alloys were used on the Spaceshattle, Ares Rockets, and the Falcon 9. Its tensile and yield strength are 595 and 505Mpa respectively. This is a much better properties compared to steel's 485 and 345 Mpa. On top of that, the density of Aluminum 2099 is 2.63 versus steels 7.8 g/cm3. This alloy's strength to weight ratio is one of the primary attributes that makes it a very appealing choice compared to steel or titanium.

SMAD recommends that all primary structures are capable of withstanding 6 g's of axial acceleration and 3 g's of lateral acceleration. This is because the forces experienced at launch will be by far the worst force that the vehicle will experience in its lifetime. Once this requirement was established, a finite element analysis was conducted for the primary structure. The team was interested to determine if using aluminum would satisfy our requirements while allowing us to save on weight. Fixed supports were added on locations of the chassis where the team anticipated the fairing supports would be connected. After this, the structure was subjected to the loads specified above. The results of this analysis can be seen in table 24. The maximum deformation of the chassis under the subjected loads came out to be .00785 mm, a very reasonable result that will more than satisfy requirements SM 3.1, 3.2, 3.3, and 3.4.

Fig. 26 Structural Analysis (View 1)

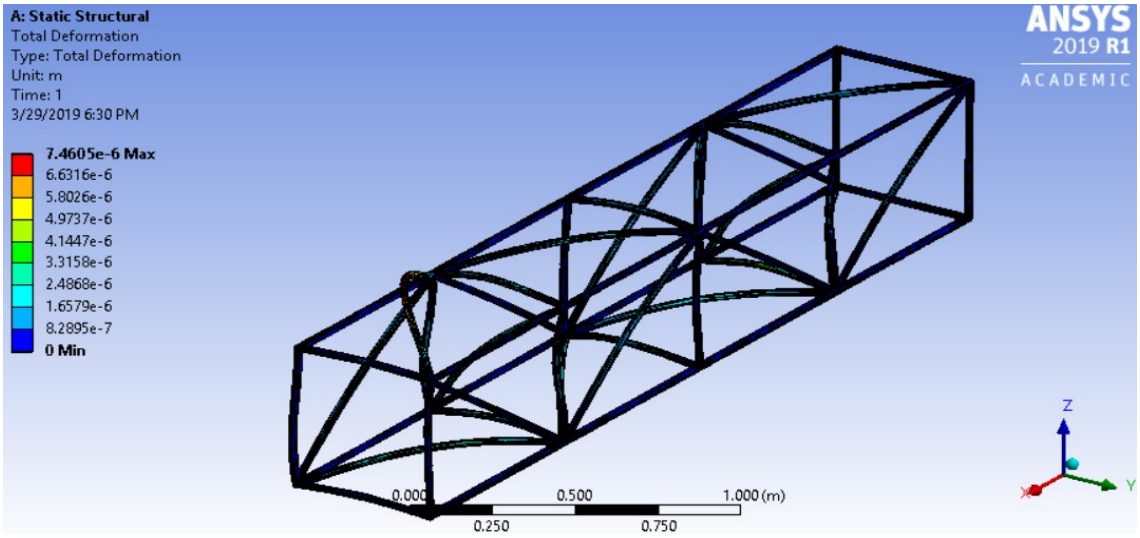

Fig. 27 Structural Analysis (View 2)

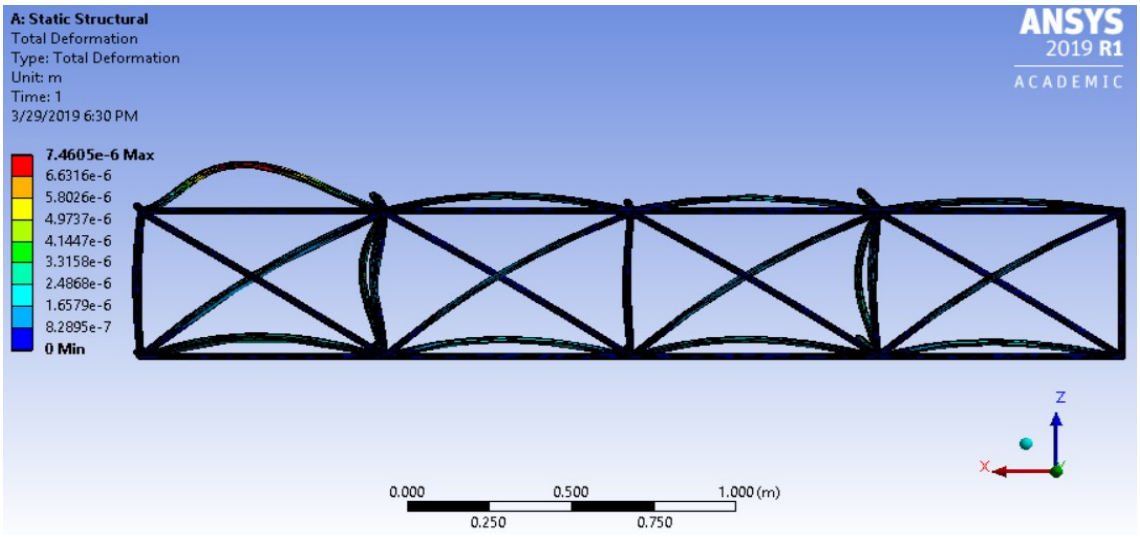

Table 14 Deformation, Stress, and Strain Results for Launch Acceleration

	6 g's Axial & 3 g's Lateral		
	Al-Li 2099	**Steel A441**	**Titanium-Alloy**
Total Deformation (mm)	0.0074605	0.008284	0.0093932
Equivalent Elastic Strain (mm/mm)	0.00001228	0.0000136	0.000015634
Equivalent Stress (KPa)	867.8	2707.7	1496.1
Mass (kg)	34.224	104.75	60.12

Table 15 Moments of Inertia

Inertia Parallel Config	
Reaction Wheel	0.000782609
Star Tracker	1.413*10^(-5)
IMU	2.61*10^(-5)
Sun Sensor	0.000217
Laser	0.005074
ROSA	0.009415
Solar Radiation	0.008922
Magnetorquers	0.008696
Horizon Sensor	1.43*10^(-5)
Power Control Unit	0.00013
Total	**0.033292**

D. Budgets

These budget tables show the allocations in each budget for all components that have been selected for the spacecraft's subsystems which contribute to those budgets.

All of the values in these tables are derived from the sources for each respective component. The components selected are identified in their respective subsystem sections.

1. Delta V

This budget is more strictly defined than the mass and power budgets, due to the limitation on hydrazine propellant carried by the spacecraft. These values were chosen using methods described in the Orbital Subsystem section for station keeping and in the End of Life discussion for the de-orbit burn.

Table 16 Delta V Budget

Contributor	Number of Maneuvers	Amount per Maneuver	Total Delta V
Station-Keeping	5	10 m/s	50 m/s
De-Orbit Thrusters	1	252 m/s	252 m/s
Total Delta V	-	-	302 m/s

2. Mass

The most significant contributing components to the mass budget are the structures, the solar panels, the Power Control Unit, and the hydrazine propellant.

Table 17 Mass Budget

Component	Mass (kg)	Quantity	Total Mass (kg)
Primary Structure	37.606	1	37.606
Secondary Structure	30 (approx)	1	30
Lasers	4.8	2	9.6
Cameras	0.036	16	0.576
Image Processing Boards	0.10	16	1.60
Startracker	0.760	4	3.04
Sun Sensor	0.375	5	1.875
Solar Panels	17.3244	2	34.6488
Power Control Unit	27.0	1	27.0
Power Distribution (Cables)	3.0	1	3.0
Magnetorquers	1.144	4	4.576
Magnetometer	0.10	2	0.20
Command Receiver	2.625	2	5.25
Transmitter	1.94	2	3.88
SSPA	1.345	2	2.690
Solar Panel Gimbal	3.462	2	6.924
Reaction Wheels	4.1	4	16.4
Hydrazine Propellant	70	1	70
Hydrazine Storage Tank	5.7	1	5.7
Infrared Earth Horizon Sensor	1.3	2	2.6
Spacecraft Management Unit	16	1	16
IMU	7.48	1	7.48
Data Storage	6.6	1	6.6
Solar Sheeting	0.351	1	0.351
Radiator	9.425	1	9.425
Li-Ion Battery	38.6	1	38.6
Total			345.62

3. Power

The laser payload instrument is by far the most power-hungry component of the craft, comprising roughly 87% of the total power consumption throughout spacecraft operation.

Table 18 Power Budget

Component	Power (W)	Quantity	Total Wattage (W)
Lasers[14]	1360	2	2720
Cameras[18]	3	16	48
Image Processing Boards[38]	10	16	160
Startracker[33]	3.25	3	9.75
Sun Sensor[34]	0.25	4	1
Spacecraft Management Unit	40-60 (Peak)	1	60
Power Control Unit[19]	20	1	20
IMU[35]	12	1	12
Command Receiver	6	2	12
Transmitter	3.5	2	7
SSPA	7	2	14
Infrared Earth Horizon Sensor	3.3	2	6.6
Data Storage[37]	10	1	10
Reaction Wheels[31] (Only 3 active)	10	4	30
Magnetorquers	1	4	4
Magnetometer[36]	1.02	1	1.02
LGA[39]	5	1	5
Total:			3120.35

E. Risk

The team was given a large amount of feedback over the various phases of the project. Many of the concerns that were raised about SWEEP were used to create this risk table. Unmitigated, the mission harbors very few risks that would result in critical or catastrophic failure modes. Regardless, the team was determined to identify what needed to be done in order to reduce the risk as much as possible. The team feels as though the risk tables below, accurately quantifies the biggest threats to the success of the mission, and clearly indicates how the team is planning on tackling them.

Fig. 28 Unmitigated Risk Assessment

Unmitigated Risk Assessment		Priority Level		
		3	2	1
		Negligible	Marginal	Critical
Likelyhood	Highly Likely to Occur .60 < P < .95			
	May Occur .20 < P < .60		Camera Misses 1mm Object Passing Through. (Frame Rate)	
	Not Likely to Occur .05 < P < .2	Propellant Accumulation On CCD/ROSA/Mirror		Laser-Mirror Misalignment Occurs During Launch/Operation

Mitigation Strategy:

For the frame rate issue, the team has oriented the cameras so that they partially eclipse the view of the cameras directly adjacent to them. It's highly likely that at least one camera will capture the event given their frame rate. The

team has acknowledged the fact that SWEEP is hindered by its camera's frame rate, and that this is likely the largest technological obstacle facing the mission. This issue is discussed heavily in the future work section.

As far as the mirror misalignment risk, the use of a rigid Aluminum Lithium Alloy 2099 chassis along with reduced mirror-to-laser to disc distance has mitigated this risk. The structural design proccess that the team went through, concluded that the most practical solution to this issue would be to use a rigid frame that uses a trusses for increased support.

In the guidance, navigation and control section, the team investigated whether or not it would be more practical to use thrusters or magnetorquers to desaturate the reaction wheels. It was concluded that the team would use magnetoquers. Fortunately, this design change reduced the amount of burn time for the mission drastically; however, the vehicle still needs to incorporate station keeping maneuvers. As a result there exists a small risk of propellant ejecta collecting on many of the onboard instruments such as the CCD's, mirrors, or the ROSA panels. This risk of accumulation may be unavoidable.

III. Problem Specific Design Solutions

A. Ground Systems Processing

To reduce the onboard complexity of the data processing for the SWEEP craft, the majority of the calculations will be computed from the ground systems. It is essential that the ground systems have all of the required information needed to perform these calculations. For these calculation, it will be assumed that the SWEEP craft will be in a circular, prograde orbit around Earth where the craft will also be pointing parallel to its forward motion at all times to ensure the maximum area of the laser disks are sweeping through space. It will also be assumed that the time between passing through two disks will be very small and the spacecraft's position does not change between these two instances. With the information from the onboard Earth sensors, it is safe to say that the left hand side of the spacecraft will always be pointing towards the center of the Earth as shown below.

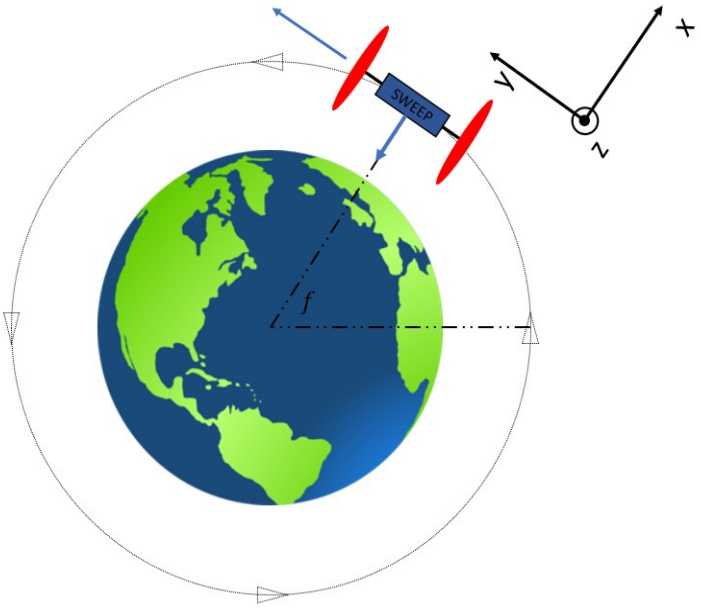

Fig. 29 SWEEP Orbit

From the craft based point of view, the coordinate system can be defined such that the x direction points directly away from the center of Earth and y points in the direction of the forward motion of the craft.

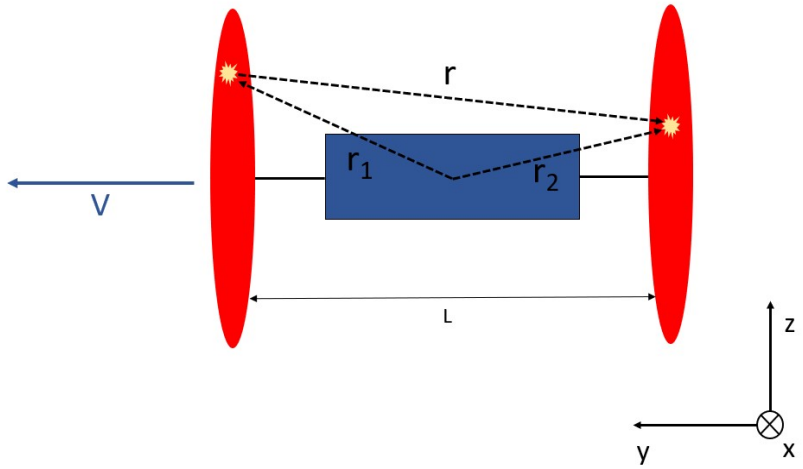

Fig. 30 Illustrated Detection Event

This spacecraft based coordinate system will help generate the velocity vector of the debris from the two points on the laser disks. For each debris detection, there will be an associated x and z point on each of the disks as well as the associated time of detection.

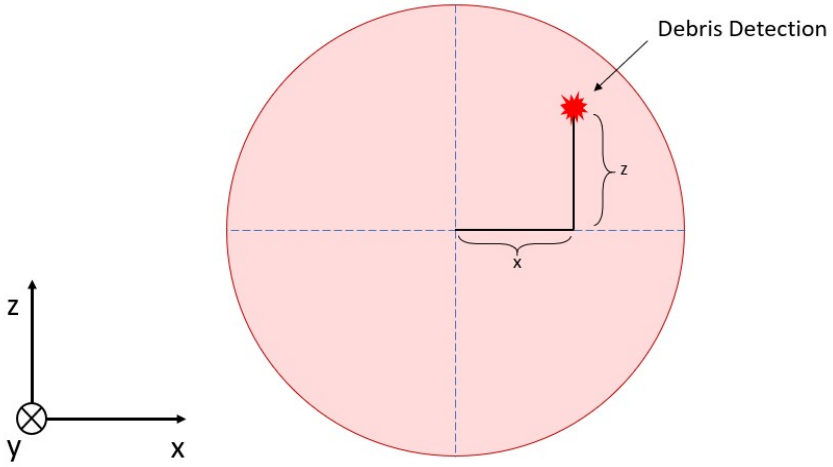

Fig. 31 Detection Coordinate on Disk

Assuming the center of the spacecraft based coordinate system is located at the center of the spacecraft, the position vector of the debris can be calculated as shown below.

The position vectors for the debris, relative to the center of the spacecraft would be:

$$\vec{r}_1 = \begin{bmatrix} x_1 \\ \frac{L}{2} \\ z_1 \end{bmatrix}$$

$$\vec{r}_2 = \begin{bmatrix} x_2 \\ -\frac{L}{2} \\ z_2 \end{bmatrix}$$

The average velocity vector of the debris relative to the spacecraft can then be defined as:

$$\vec{v}_{avg} = \frac{\vec{r}_2 - \vec{r}_1}{\vec{t}_2 - \vec{t}_1}$$

$$\vec{v}_{avg} = \frac{\begin{bmatrix} (x_2 - x_1)\hat{i} & (-L)\hat{j} & (z_2 - z_1)\hat{k} \end{bmatrix}}{\Delta t}$$

These calculation were made assuming the spacecraft was not rolling around the y-axis, and the center of the Earth was directly to the left of the spacecraft. In reality this will not be the case, however it can be corrected using the onboard Earth sensors.

The problem then becomes transferring the position vector from the spacecraft to the debris in the spacecraft coordinate frame to the position vector from the Earth to the debris in the Earth centered reference frame.

This can be possible given the points of impact on each of the disks, radius of the orbit, and the orbital elements of the spacecraft.

From the spacecraft centered reference frame defined above, the position vector from spacecraft to debris is defined as:

$$\vec{r}_{sd} = \begin{bmatrix} x_2 - x_1 \\ -L \\ z_2 - z_1 \end{bmatrix}$$

To transfer this to the Earth centered inertial (ECI) reference frame, it must be transferred to the perifocal point of view. This point of view is in the place of the spacecraft's orbit and is illustrated below. Transferring from the spacecraft reference frame to the perifocal reference frame can be done by rotating around the z-axis.

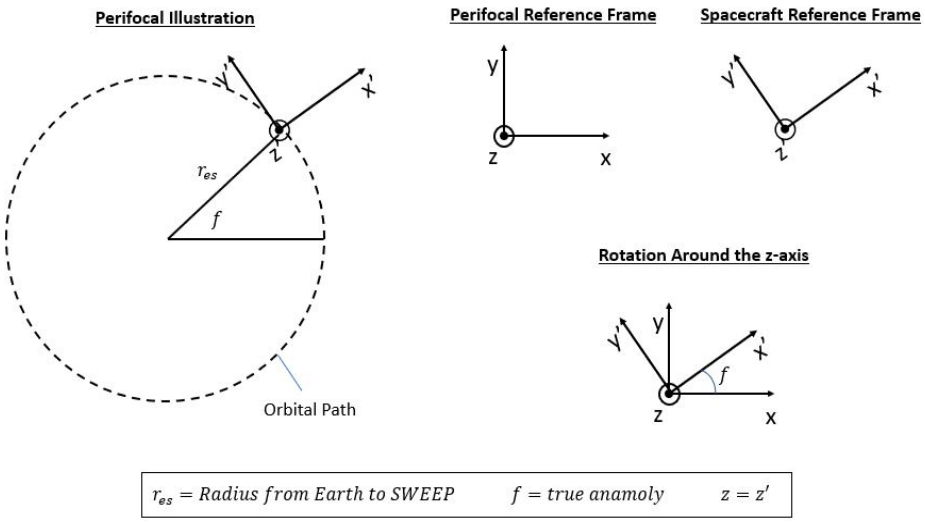

$r_{es} = Radius\ from\ Earth\ to\ SWEEP \qquad f = true\ anamoly \qquad z = z'$

To transition from the spacecraft to the perifocal reference frame, a z-axis rotation matrix can be used as shown below.

$$R_z(f) = \begin{bmatrix} cosf & -sinf & 0 \\ sinf & cosf & 0 \\ 0 & 0 & 1 \end{bmatrix}$$

This will then give the position of the space debris from the spacecraft in the perifocal reference frame.

$$\vec{R}_{psd} = \begin{bmatrix} cosf & -sinf & 0 \\ sinf & cosf & 0 \\ 0 & 0 & 1 \end{bmatrix} * \vec{r}_{sd}$$

$$\vec{R}_{psd} = \begin{bmatrix} cosf & -sinf & 0 \\ sinf & cosf & 0 \\ 0 & 0 & 1 \end{bmatrix} * \begin{bmatrix} x_2 - x_1 \\ -L \\ z_2 - z_1 \end{bmatrix}$$

Now we know the position vector from the Earth to the spacecraft as well as the position vector from the spacecraft to the debris, both of which are in the perifocal frame. The position vector from the Earth to debris can then be solved simply by adding the two vectors.

$$\vec{R}_{ped} = \vec{r}_{es} + \vec{R}_{psd}$$

Where the position vector from Earth to spacecraft in perifocal reference frame is defined as shown.

$$\vec{r}_{es} = \begin{bmatrix} rcosf \\ rsinf \\ 0 \end{bmatrix}$$

Finally, the position vector $\vec{R}_{ped}$ can then be converted into the ECI reference frame by multiplying by the transformation matrix defined below.[41]

$$\vec{R}_{PQW \to ECI} = \begin{bmatrix} cos\Omega & -sin\Omega & 0 \\ sin\Omega & cos\Omega & 0 \\ 0 & 0 & 1 \end{bmatrix} \begin{bmatrix} 1 & 0 & 0 \\ 0 & cos\, i & -sin\, i \\ 0 & sin\, i & cos\, i \end{bmatrix} \begin{bmatrix} cos\omega & -sin\omega & 0 \\ sin\omega & cos\omega & 0 \\ 0 & 0 & 1 \end{bmatrix}$$

The same calculations can be performed for the velocity of the debris. Starting with the velocity vector from the spacecraft to the debris in the spacecraft's reference frame.

$$\vec{v}_{sd} = \frac{1}{\Delta t} * \begin{bmatrix} x_2 - x_1 \\ -L \\ z_2 - z_1 \end{bmatrix}$$

This is then rotated into the perifocal reference frame by rotating around the z-axis.

$$\vec{V}_{psd} = \begin{bmatrix} cosf & -sinf & 0 \\ sinf & cosf & 0 \\ 0 & 0 & 1 \end{bmatrix} * \vec{v}_{sd}$$

$$\vec{V}_{psd} = \begin{bmatrix} cosf & -sinf & 0 \\ sinf & cosf & 0 \\ 0 & 0 & 1 \end{bmatrix} * \begin{bmatrix} x_2 - x_1 \\ -L \\ z_2 - z_1 \end{bmatrix} * \frac{1}{\Delta t}$$

Adding the velocity vector from Earth to spacecraft to the velocity vector from the spacecraft to the debris in the perifocal reference frame.

$$\vec{V}_{ped} = \vec{V}_{es} + \vec{V}_{psd}$$

Where the velocity vector from the Earth to spacecraft and the velocity of the circular orbit are defined below.

$$\vec{V}_{es} = \begin{bmatrix} -vsinf \\ vcosf \\ 0 \end{bmatrix}$$

$$v = \sqrt{\frac{\mu_{earth}}{r}}$$

Finally, the last step is to convert this vector from the perifocal reference frame to the ECI reference frame by multiplying by the transformation matrix listed above.

$$\vec{V}_{ed} = \vec{R}_{PQW \rightarrow ECI} * \vec{V}_{ped}$$

This process was then coded in matlab and used to generate the figure of a sample calculation below, proving that the data collected by the spacecraft will be sufficient to map the position and velocity vectors of space debris.

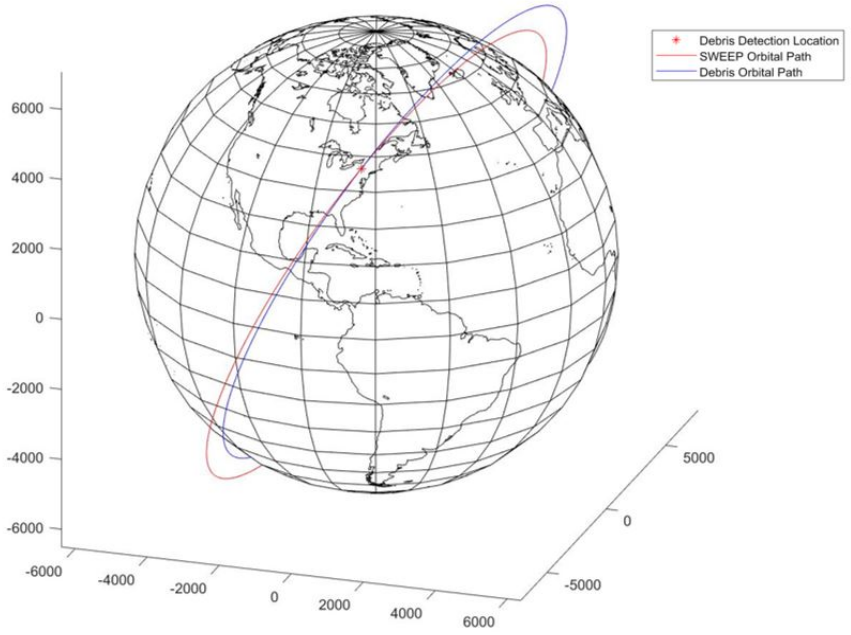

Fig. 32 Orbital Trajectory of SWEEP and Debris

B. Uncertainty in Orbital Calculations

The uncertainties in the measurement of the debris' disk intersection varies with the distance from the spacecraft due to the pixels increasing FoV. Should a piece of debris illuminate a pixel the debris will be anywhere within its FoV, thus the uncertainty is the height and width of the pixel. The uncertainty in the disk transverse time measurement is defined by the frame rate of the sensors.

$$\sigma t = \pm 200ns$$

The maximum size pixel width:

$$\sigma x_{max} = \pm 0.0021m$$

Pixel heights at 500, 250, and 10 meters from space craft:

$$\sigma z_{@500m} = \pm 0.005m$$

$$\sigma z_{@250m} = \pm 0.00113m$$

$$\sigma z_{@10m} = \pm 0.00077m$$

To calculate the uncertainties in the orbital elements, the values above were evaluated using method outlined in Ground system processing.

Using the code mentioned above to plot the debris, the maximum and minimum values were input, which would output the position and velocity vectors for each instance. The difference between these values was then calculated to observe how much of an effect this error would cause on the final vectors. This error is shown below in the tables for 10, 250, and 500 meter radius from the spacecraft.

Table 19 Error in Position Vector

	10 m	**250 m**	**500 m**
x	1.36E-05	1.99E-05	8.81E-05
y	2.39E-06	3.50E-06	1.55E-05
z	6.90E-05	1.01E-05	4.48E-05

Table 20 Error in Velocity Vector

	10 m	**250 m**	**500 m**
x	1.36E-03	1.99E-03	8.81E-03
y	2.39E-04	3.51E-04	1.55E-03
z	6.90E-04	1.01E-03	4.48E-03

C. Environmental Analysis and Design Considerations

Desaturation Methods One of the biggest challenges to creating a spacecraft that has a net positive effect on the presence of space debris, is ensuring that your own vehicle does not create more problems than it solves. In the beginning of the project the team knew that SWEEP would need to have the ability to rotate and orient itself accordingly. The easiest design solution to this was desaturation thrusters. This was the go-to because it quickly and conveniently solved the issue of attitude control. However, the more the team looked into this option, the more it became apparent that if de-sat thrusters were indeed going to be used, SWEEP would need to desaturate something on the order of 56 times per day. Not only did this become impractical, it became an environmental concern. Dozens of kilograms of propellant would be needed to pull this off. Firing thrusters this often, while in a consistent orbit would only add to the mess of low earth orbit. After the trade off between de-sat thrusters and magnetorquers, the team was very relieved that SWEEP would no longer need to create clouds of propelanet in order to orient itself.

Laser Intensity One of the larger concerns that was brought forth to the team multiple times, was the fact that SWEEP is indeed blasting two 100W lasers into low Earth orbit, where thousands of other vehicles reside. Is there a chance that this laser could interfere with many of the other spacecraft in the region? What if one were to pass through this laser? Would its systems be damaged at all? Fortunately the design requirements of the project lead the group to use a laser with a very high wavelength. This wavelength is ideal for SWEEPs cameras system since it would need to ignore interferences created by the Sun.

As far as the intensity goes, one should keep in mind that the laser is being diffused in 360 degrees by the conical mirror. As a result it is significantly weakened, and would drop off even more with distance. The OODS report that was discussed in the payload section, enabled the group to calculate the amount of photons that SWEEP can expect to receive back when an object passes through the laser. If SWEEP itself will be using all of its onboard systems to retrieve the small amount of photons being produced by the scattering event, then the team anticipates that the laser would have no noticeable effect on a spacecraft that passed even within 1km of SWEEP, especially considering that it would only take a fraction of a second for it to pass through the lasers path.

End of Life Even within the first few days after beginning the project, the team knew that it would be highly unethical to simply leave SWEEP drifting in orbit after it had served its primary function. The most logical answer to the end of

life plan for SWEEP was to directly deorbit itself into the ocean from 900km. This is the current end of life plan. There were however, other options that were being considered over the course of the design process.

While working out the details to the end of life plan, attention was given to how much propellant can and should be used to deorbit the vehicle. The team is very aware that the environment that SWEEP occupies is a relatively chaotic one, possessing a large number of disturbances that will alter the orbit of SWEEP: solar pressure, gravitational gradients, J2 perturbations, aerodynamic forces, electromagnetic disturbances, and tidal forces from the moon and sun are a few examples of what SWEEP will encounter. One of the early deorbiting plans involved using these disturbances to assist the deorbiting proccess. This first alternative option was to do a direct Hohmann burn down to an altitude of about 200km and let the significant drag forces take care of the rest. Ground stations monitoring the event would be able to verify that the reentry trajectory is on course for a safe, remote location in the ocean. This method reduces the fuel that SWEEP would have to expend in order to deorbit.

Another strategy which could also be value added to the mission, would be to allow SWEEP to skip the last several station keeping burns. Doing this will change the orbital trajectory, and for a limited time, SWEEP will be able to access new altitudes, and possibly even obtain new debris data that it would not have discovered at its previous altitude. This descent to a lower altitude must be carefully monitored; as there is no doubt it would cross through the parking orbit altitudes of other spacecraft. If this method was selected, SWEEP would allow its orbit to decay for a number of weeks, or possibly years, and then finally use its de-orbiting thrusters to bring itself directly into a controlled reentry. Ultimately, the first option discussed was chosen due to the complications and logistics of the latter two options. The team has determined that a direct controlled deorbit into the ocean is by far the most practical, ethical, and safest way to end SWEEP's mission.

IV. Conclusions

A. Current Issues

Over the course of this project, many calculations, modeling, and trade studies have been completed to meet the defined requirements. Although there has been great progress, the end of the semester has come and there are a few current issues that have not yet been resolved.

One of the major outstanding issues is with regards to the sampling frequency that is needed to ensure all debris passing through the laser can be detected. The details of the subsystems were based on a very low shutter speed of 18 fps. However, the required value has been calculated and shows that the camera must be able to take a picture every 200 ns to ensure all debris detections are recorded. This then dramatically changes the onboard processing and power consumption. The current system in place with only 18 images taken a second creates a large risk of the debris passing through the disk undetected.

A few possible solutions have been listed below:

1) Increase the distance between the two laser disks by having two spacecraft, each with its own laser disk. The larger separation would allow lower shutter speeds for velocity calculations.
2) Increase the image processing power. This could possibly be done with ASIC.
3) Use a more improved camera or develop new methods for data collection.

The team acknowledges that this is a significant point of concern, however there is no doubt that this may be mitigated entirely by future technology that would enable SWEEP to have a high frame rate, well beyond 5 million frames per second while having the necessary onboard processing power. In a matter of years this technology may be very practical and inexpensive to use on a spacecraft.

B. Future Work and Continued Development

Finally, it becomes noticeable that there are still many details that need to be considered and worked on before the concept can be fully developed. Up to this point, the main focus has remained fixed on the actual debris detection devices ensuring they meet the main requirements of the project. The details of the critical subsystems have also been worked through, however have not completely finalized. The following list shows the future work that would need to be done to fully complete this project.

1) Reduce the overall size and weight of the spacecraft, given improved equipment and optimized design.
2) Select a more optimized processor for image processing. This would allow for a better way to see light from debris detection

3) Find a better camera, sensor, or process that would resolve the shutter speed issue mentioned above in the current issues section.
4) Create a constellation of satellites with the optimized spacecraft design to map out other orbits.

V. Appendix

A. Subsystem Requirements

Table 21 Payload Requirements

No.	Requirement	Rationale	Required Value	Expected Value	Verification Method
DDTS-3.1	Payload shall detect particles in size of 1mm to 10cm within 500 m of spacecraft(s)	Current instruments are unable to detect debris smaller than 1 cm.	1mm to 10cm within 500 m.	1mm within 5m 1cm within 50m10cm within 500m	Test
DDTS-3.2	The laser shall have an optical power of 100 Watts	Required value to measure 10cm debris at 500m	100 Watts	100 Watts	Test
DDTS-3.3	The laser shall have a wavelength greater than 3000nm	The Sun emits near zero at that above this wavelength (less noise)	>3000nm	10600 nm	Test
DDTS-3.4	The conic mirror shall have a reflectance of 95% or greater at selected wavelength	To minimize wasted optical power	>=95%	98%	Test
DDTS-3.5	The sensors shall measure the measure a band ±2% around the selected wavelength	To minimise noise to sensor	±15%	±11%	Test
DDTS-3.6	The selected filter shall emit >= 90% of the selected wavelength	To minimize wasted optical power	>= 90%	0.92	Test
DDTS-3.7	The payload shall detect objects traveling at speed 15km/s and less relative to spacecraft	Orbital velocity at 1000km is 7.35 km/s so an object in a retro-orbit would be ~15km/s relative to spacecraft	<= 15km/s	<= 15km/s	Test
DDTS-3.8	The payload shall measure debris disk to disk time with +/- 200ns	Required to find the relative orbital velocity of passing debris	+-200ns	+-200ns	Test
DDTS-3.9	The sensor shall measure the location of the debris, relative to spacecraft, with an uncertainty of +/- 0.5cm	Required to find the orbital positions of passing debris	+/- 0.5cm	+/-0.5cm	Test

Table 22 Power Requirements

No.	Requirement	Rationale	Required Value	Expected Value	Verification Method
EPS - 3.1	Power systems shall provide continuous uptime for instruments.	In fulfillment of MO-1.1 and 2.2, detection payload shall remain powered throughout the mission, even while the spacecraft passes through the umbra produced by the Earth, to detect as many debris objects as possible.	3590W + 42W excess generated by ROSA while in sunlight through end-of-life.	3590W + 528.8W excess generated by ROSA while in sunlight at end-of-life.	Test during sunlight exposure.
EPS-3.2	Spacecraft shall retain sufficient power to deorbit at end-of-life.	In fulfillment of MO-1.4, must maintain electrical operation through end-of-life.	<5% Solar Panel Efficiency decay per year over lifetime. (BOL)	~1% Solar Panel Efficiency decay per year over lifetime. (BOL)	Analysis

Table 23 Guidance, Navigation and Control Requirements

No.	Requirement	Rationale	Required Value	Expected Value	Verification Method
GNC 3.1	The attitude control system shall maintain a level of accuracy on the order of <360 arc seconds while the laser is operational.	The payload is extremely precise and even one degree difference can produce a drastically different trajectory	<360 arc seconds	360 arc seconds	Testing

Table 24 Thermal Requirements

No.	Requirement	Rationale	Required Value	Expected Value	Verification Method
TCS-3.1	Thermal systems shall maintain subsystem temperatures within the limits required by subsystem manufacturers.	Keeping subsystem temperatures within limits allows the spacecraft to have optimum performance.	10ºC to 30ºC	10ºC to 20ºC	Analysis

Table 25 Orbital Requirements

No.	Requirement	Rationale	Required Value	Expected Value	Verification Method
OR-3.1	Spacecraft shall be placed in an orbit useful to future US Based Spacecraft.	The tracking of debris is most valuable for mitigation of risk to current and future U.S. satellites.	63.4 deg (Critical Inclination)	63.4 deg	Demonstration
OR-3.2	Spacecraft shall be placed where Orbital Debris Density is highest.	This tracking data is also more useful if more debris objects can be detected from the orbit of the SWEEP satellite, therefore an orbit with more dense debris is preferable.	900 km	900 km	Demonstration
OR-3.3	SWEEP shall Maintain a Circular Orbit	A circular orbit will give us the best survey of data and will demonstrate	<0.05 eccentricity	<0.01 eccentricity	Demonstration
OR-3.4	Orbit shall be maintained to account for appropriate perturbations.	Over time, drag, J2 and Solar Radiation Pressure, a well as tidal forces will alter our orbit. This must be compensated for.	10m/s Orbital Decay per year	10m/s	Calculations

Table 26 Propulsion Requirements

No.	Requirement	Rationale	Required Value	Expected Value	Verification Method
PR - 3.1	Spacecraft shall retain sufficient fuel to deorbit at end-of-life.	In fulfillment of MO-1.4, must retain sufficient propellant to reduce periapsis into atmosphere to deorbit.	252 m/s ΔV and 50 kg of Hydrazine	50 kg of Hydrazine	Analysis
PR - 3.2	Spacecraft thrusters shall maintain desired orbit throughout mission life.	Must perform station keeping to correct orbit perturbations.	50 m/s ΔV and 12 kg of Hydrazine	12 kg of Hydrazine	Demonstration

Table 27 Command and Data Handling Requirements

No.	Requirement	Rationale	Required Value	Expected Value	Verification Method
CDH-3.1	Shall reserve data for on board image processing	Needs to store data to enable SMU to process data	3600Mb	128Gb	Analysis
CDH-3.2	Shall have enough onboard storage for 3 orbits worth of data	Have excess storage in case transmission is missed	3600Mb	128Gb	Analysis
CDH-3.3	Shall process data to select only relevant images and data	Dramatically reduce onboard storage and communication requirements	<4 images per detection event	<3 images per detection event	Analysis
CDH-3.4	Shall reserve data to store relevant spacecraft health and status information	Needed to monitor and track the life of the system	100Mb/Orbit	1000Mb/Orbit	Analysis

Table 28 Communication Requirements

No.	Requirement	Rationale	Required Value	Expected Value	Verification Method
COM-3.1	Shall send all stored data to ground systems once every orbit	Dump data so large amount of data storage is not required	90 kbps	90 kbps	Analysis
COM-3.2	Shall be able to receive commands from ground stations each orbit with a data rate of 10 kbps	Must have the opportunity to update or control satellite from ground station	10 kbps	10 kbps	Analysis

Table 29 Structures and Mechanisms Requirements

No.	Requirement	Rationale	Required Value	Expected Value	Verification Method
SM 3.1	The primary structure (load baring) of SWEEP must be able to survive and function, while undergoing loads induced by the launch vehicle.	The forces experienced at launch are the most intense.	6 g's maximum axial acceleration, 3 gs maximum lateral acceleration	8g's and 4.5 g's respectively. FOS (1.5)	FEA and Failure Mode Analysis
SM 3.2	The secondary structure of SWEEP must be able to survive the loads induced by the launch vehicle.	The Secondary structure such as sensor mounting does not need to operate during the launch, it must only survive it.	6 g's maximum axial acceleration, 3 g's maximum lateral acceleration	8g's and 4.5 g's respectively. FOS (1.5)	FEA and Failure Mode Analysis
SM 3.3	SWEEP shall have a total primary and secondary structural mass between 10% to 20% of the spacecraft dry mass.	This includes the bus structure, equipment/sensor housing, and mounts.	10% to 20%	64.7kg (12.94%)	Analysis
SM 3.4	The internal Volume of SWEEP shall be large enough to store 306.9m/s of delta V.	SWEEP must be able to carry enough onboard delta V to deorbit and perform station keeping for at least 5 years.	67.73 liters	91.44 liters (346.49 m/s)	Space Allocation Analysis
SM 3.5	The Primary and Secondary Structure shall have strength and stiffness properties that will minimize pointing error caused by vibrational modes.	The alignment of the laser-mirror set up is crucial to the missions success. The vehicle must stay aligned at all times since it will be rotating at all times.	Pointing error caused by vibrational modes shall be no greater than 360 arcseconds. (.1) degree.	360 arcseconds	FEA and Failure Mode Analysis

B. Requirement Tracking

Requirements are what drive the entire mission. Since requirements are vitally important, a requirement tracking table was made to point to sections where the team believes a requirement was met. The first column represents the requirement number and the second column represents where in the text a requirement was achieved. For higher level requirements a subsection and page number are provided. For subsystem requirements a specific area of the subsection (when available) and page number are provided.

Table 30 Requirements Tracking

Req No.	Location Satisfied	Pg. No.	Req No.	Location Satisfied	Pg. No.
MO-1.1	1.Payload	Pg. 22	OR-3.1	2.Orbital Conditions and Determination	Pg. 21
MO-1.2	3.Launch Systems and Propulsion	Pg. 27	OR-3.2	2.Orbital Conditions and Determination	Pg. 21
MO-1.3	6.Command and Data Handling	Pg. 36	OR-3.3	Orbital Calculations	Pg. 22
MO-1.4	3.Launch Systems and Propulsion	Pg. 25	OR-3.4	Orbital Calculations	Pg. 23
MO-1.5	B. Concept of Operations	Pg. 7	PR-3.1	3. Launch Systems and Propulsion	Pg. 24
DDTS-3.1	Laser Optical Power	Pg. 10	PR-3.2	3. Launch Systems and Propulsion	Pg. 24
DDTS-3.2	Laser Optical Power	Pg. 10	CDH-3.1	6. Command and Data Handling	Pg. 32
DDTS-3.3	Laser	Pg. 9	CDH-3.2	6. Command and Data Handling	Pg. 32
DDTS-3.4	Conic Mirror	Pg. 11	CDH-3.3	6. Command and Data Handling	Pg. 32
DDTS-3.5	Filter	Pg. 14	COM-3.1	7. Communications System	Pg. 34
DDTS-3.6	Filter	Pg. 14	COM-3.2	7. Communications System	Pg. 36
DDTS-3.7	Sampling Frequency	Pg. 13	SM-3.1	Material	Pg. 45
DDTS-3.8	Sampling Frequency	Pg. 14	SM-3.2	Material	Pg. 45
DDTS-3.9	Focal-Plane Array	Pg. 13	SM-3.3	Material	Pg. 46
EPS-3.1	Power Source	Pg. 27	SM-3.4	Space Allocation	Pg. 45
EPS-3.2	Power Storage	Pg. 27	SM-3.5	Material	Pg. 45
GNC-3.1	8.GNC	Pg. 36	TCS-3.1	5.Thermal	Pg. 30

C. Project Management

Role Assignment Roles were assigned based off of the eight different subsystems of the spacecraft. These subsystems were assigned both a primary and secondary worker. Often there were multiple assigned secondaries to help with a complex subsystem. The role assignment breakdown can be seen below.

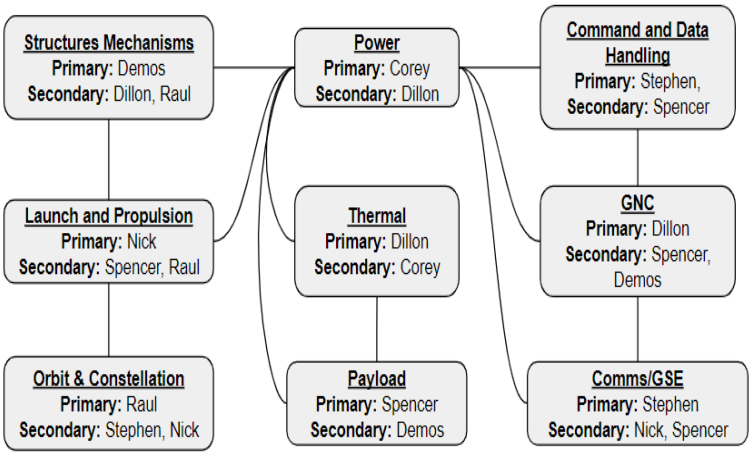

Fig. 33 Role Assignment Breakdown

Scheduling and Gantt Chart The following figures layout the timeline for all tasks.

WBS#	TASK TITLE	TASK OWNER	START DATE	DUE DATE	DURATION	Completion
1	**Project Conception and Initiation**					
1.1	Project Charter	Team	1/14/201	1/11/2019	5	100%
1.2	Mission Statement	Team	1/21/201	1/11/2019	10	100%
1.3	Define Requirments	Team	1/17/201	3/21/2019	7	100%
1.4	Distribute Roles & Responsibilites	Team	1/22/201	2/8/2019	10	100%
1.5	Trade: Instrument Choice	Team	1/15/201	2/6/2019	12	100%
1.6	Trade: Parking Orbit	Demos	1/28/201	2/5/2019	9	100%
1.7	Determine Power Req of Laser	Stephen & Correy	1/18/201	1/31/2019	6	100%

WBS#	TASK TITLE	TASK OWNER	START DATE	DUE DATE	DURATION	Completion
1	**Project Conception and Initiation**					
2	**Project Definition and Planning**					
2.1	Chose Solar Arrays	Correy	2/7/2019	2/26/2019	14	100%
2.2	Determine Attitude Control Method	Dillon & Demos	2/14/201	2/21/2019	6	100%
2.3	Create a Concept Design	Demos, Correy	2/4/2019	2/15/2019	10	100%
2.4	Create CONOPS	Stephen	2/18/201	2/12/2019	3	100%
2.5	Define Major System Requirments	Everyone	2/11/201	2/21/2019	9	100%
2.6	Subsystem Element Requirements	Team	2/19/201	3/11/2019	15	100%

WBS#	TASK TITLE	TASK OWNER	START DATE	DUE DATE	DURATION	Completion
1	**Project Conception and Initiation**					
2	**Project Definition and Planning**					
3	**Project Conception and Initiation**					
3.1	Determine Desaturation Method	Demos, Dillon	2/11/19	2/20/2019	8	100%
3.2	Determine Eclipse Time	Correy	2/20/19	2/20/2019	1	100%
3.3	Determine Comms Blackout	Correy	2/18/19	2/21/2019	4	100%
3.4	Determine Number of Cameras Needed	Spencer	2/12/19	2/28/2019	14	100%
3.5	Determine Camera Blind Spots	Spencer	2/13/19	3/12/2019	20	100%
3.6	Mass of Laser Emitter	Spencer	3/4/19	3/8/2019	10	100%
3.7	Determine Neccessary Storage Capcity	Correy	3/8/19	3/12/2019	3	100%
3.8	Determine Comms Blackout time	Correy	3/7/19	3/8/2019	7	100%
3.9	Determine Comms Antenna Size	Correy	3/12/19	3/18/2019	5	100%
3.1	Determine Thermal Operating Range	Dillon	3/18/19	3/26/2019	7	100%
3.11	Thermal Control Method	Dillon	3/19/19	3/26/2019	6	100%
3.12	Determine Fuel Needed	Nick Raul	3/18/19	3/26/2019	7	100%
3.13	End of Life Plan	Nick	3/17/19	3/19/2019	3	100%
3.14	Space Allocation Analysis	Team	3/8/19	3/25/2019	12	100%
3.15	Create Visualization of Spacecraft	Team	3/18/19	3/25/2019	6	100%
3.16	Structural Analysis	Demos	3/20/19	3/29/2019	8	100%
3.17	Create System Archetectural Breakdown	Team	3/15/19	3/28/2019	10	100%
3.18	Estimate Mission Cost	Demos	3/26/19	3/28/2019	3	100%

WBS#	TASK TITLE	TASK OWNER	START DATE	DUE DATE	DURATION	Completion
1	**Project Conception and Initiation**					
2	**Project Definition and Planning**					
3	**Project Conception and Initiation**					
4	**Project Performance/Conclusion**					
4.1	Satisfy all Subsystem Reqs	Team	3/26/19	4/2/2019	6	100%
4.2	Verification and Validation	Team	3/27/19	3/29/2019	3	10%
4.3	Future Considerations	Team	3/28/19	4/1/2019	3	25%
4.4	Lessons Learned	Team	3/29/19	4/2/2019	3	20%
4.5	Formatting	Team	3/26/19	4/4/2019	8	30%
4.6	Citations & Referances	Team	4/1/19	4/3/2019	3	40%
4.7	Final Presentation/Report	Team	4/1/19	4/29/2019	18	30%

D. N^2 Diagram

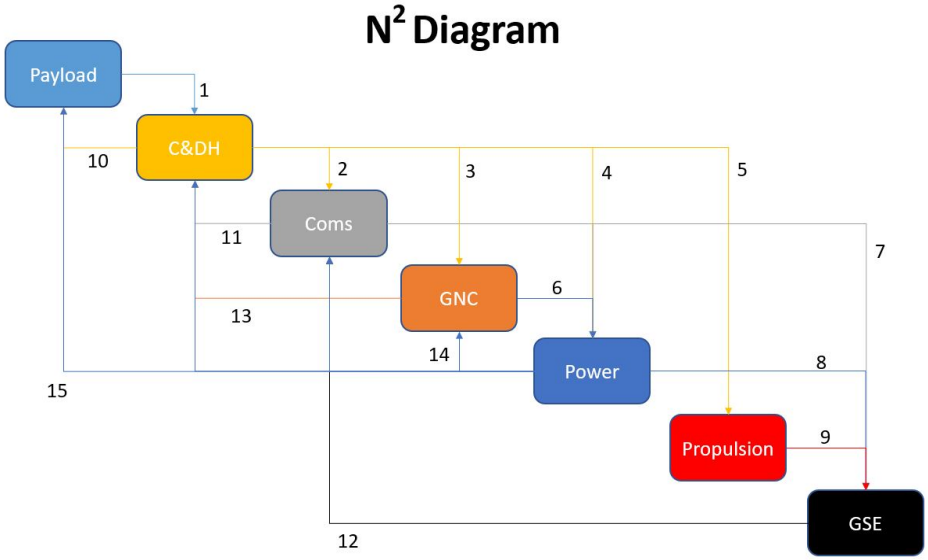

Table 31 N^2 Details

Number	From	To	Details
1	Payload	C&DH	Debris Detection Data
2	C&DH	Coms	Processed/Filtered Data
3	C&DH	GNC	Execute Maneuvers
4	C&DH	Power	Hard Disk
5	C&DH	Propulsion	Maneuvers
6	C&DH	Payload	Payload Controls
7	Coms	GSE	Send Filtered Data
8	Coms	C&DH	Maneuvers / Updates
9	GNC	Power	Sun Tracker/Reaction Wheels
10	GNC	C&DH	Guidance
11	Power	GSE	Analysis/Verification
12	Power	GNC	Power Distribution
13	Power	Payload	Laser Power
14	Propulsion	GSE	Analysis/Verification
15	GSE	Coms	Maneuvers / Updates

E. CAD Renderings

1.
Dimensions of SWEEP Chassis

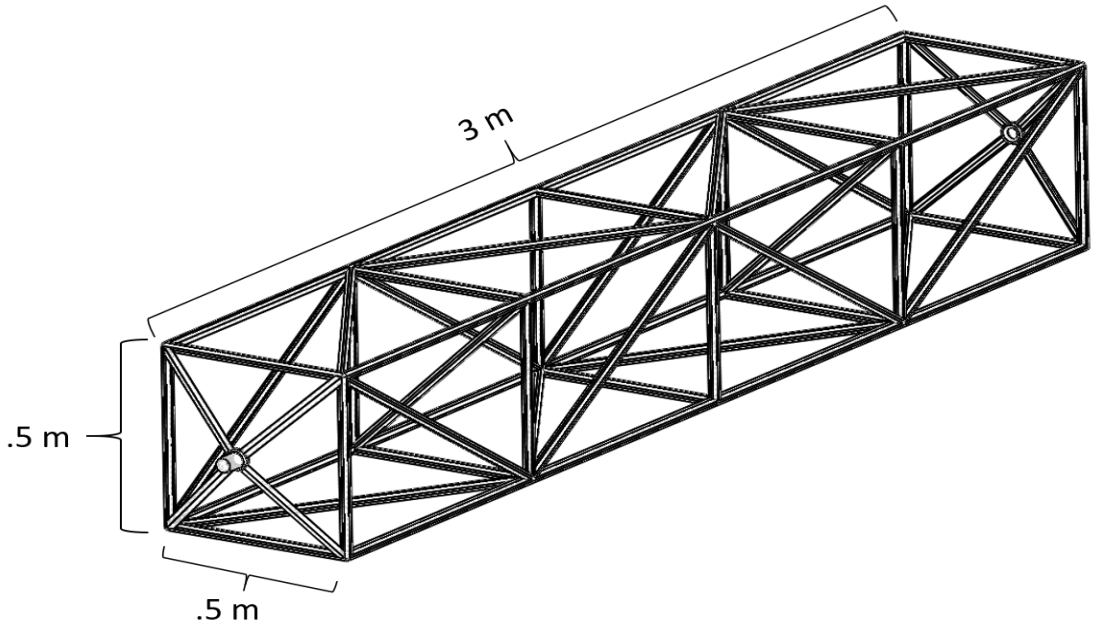

2. *Top, Side and Front View of SWEEP*

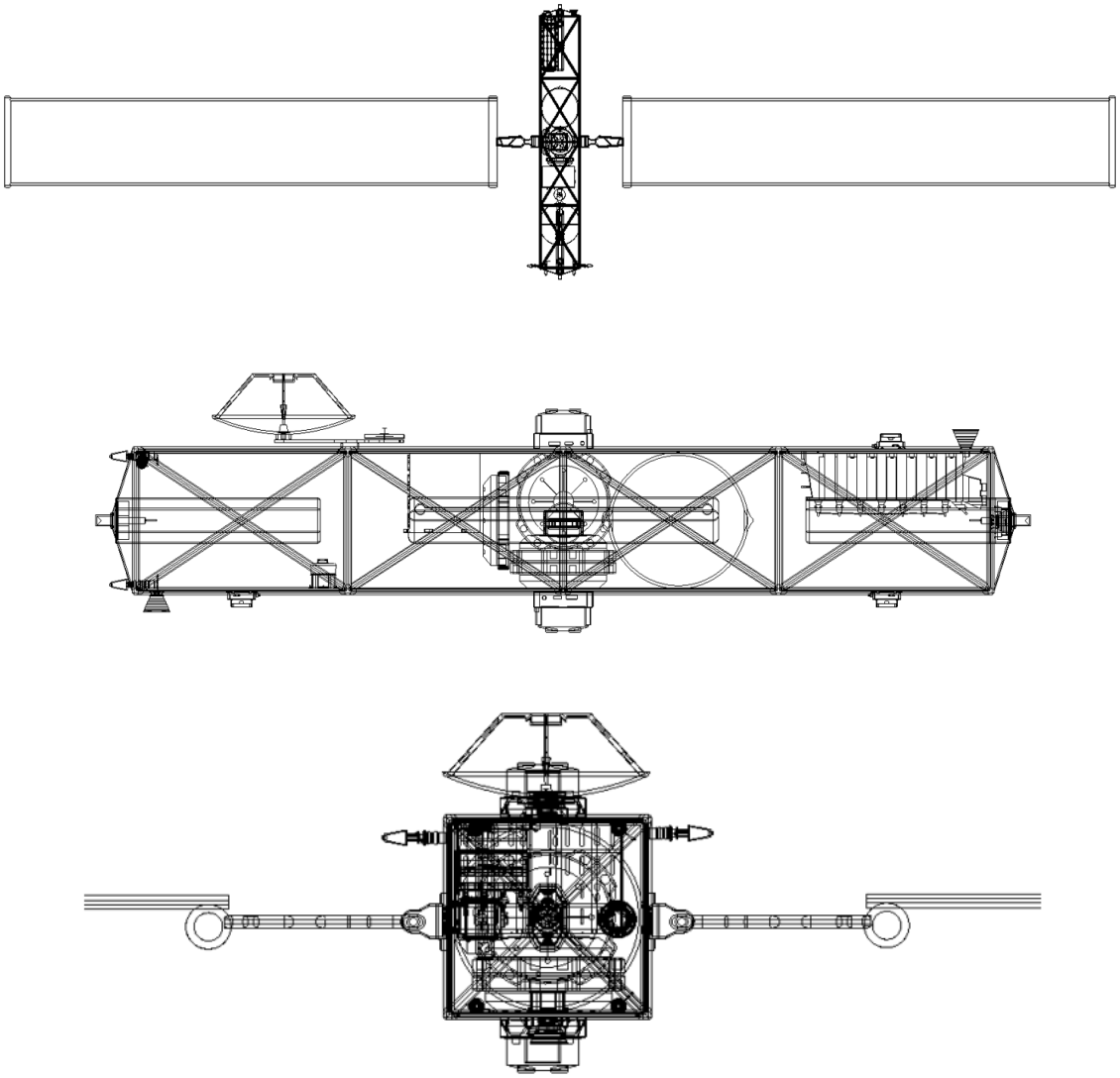

3. *Side View*

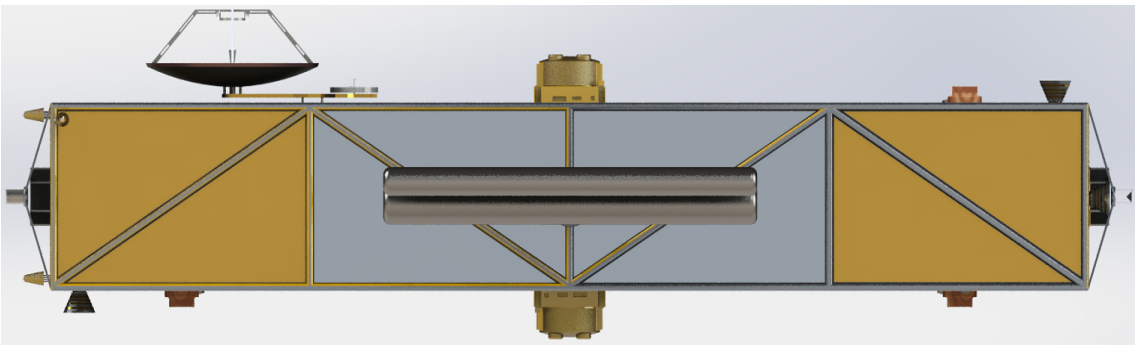

4. Laser/Mirror Setup

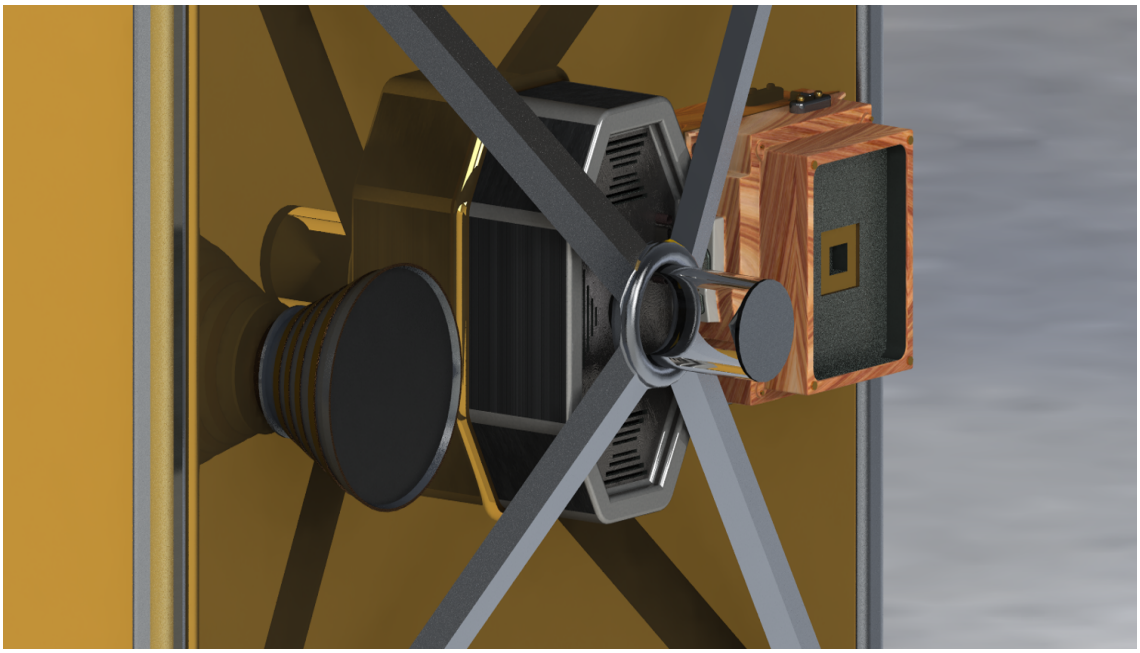

5. The Components of SWEEP

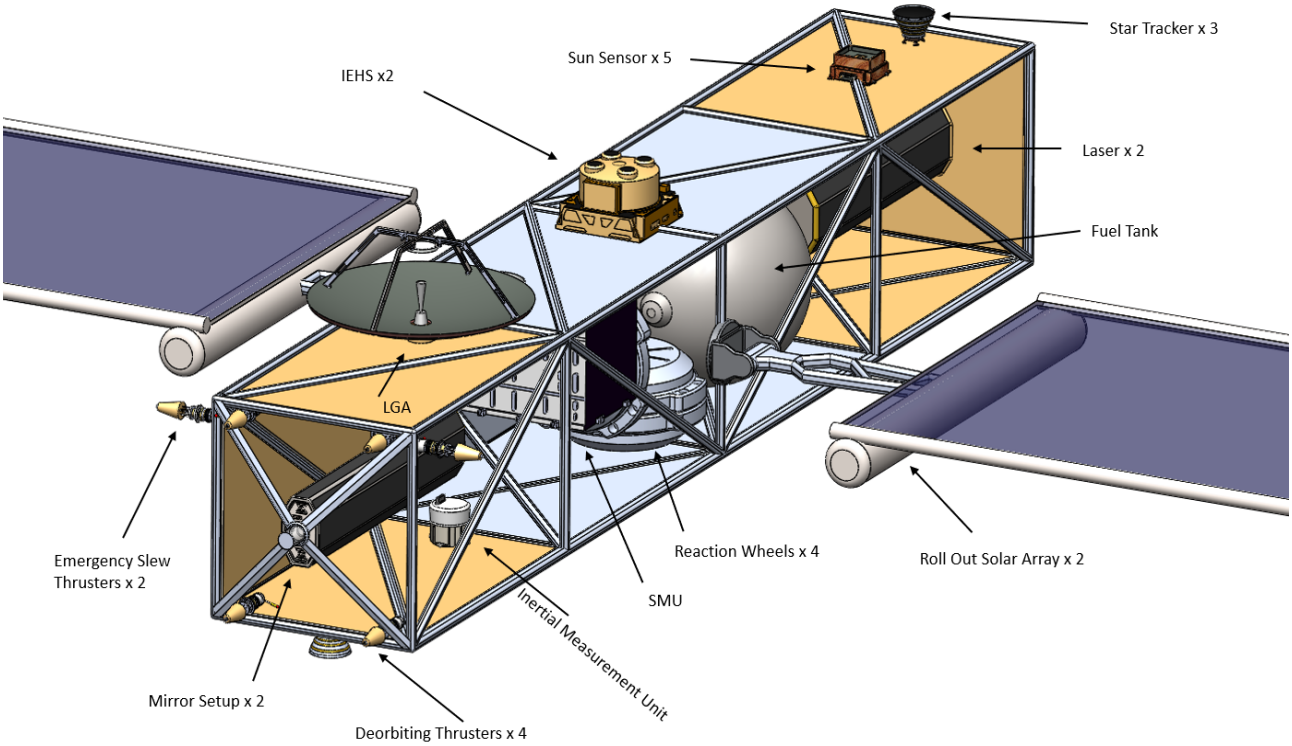

References

[1] Wade, M. (2017). IS-A. Astronautix. Retrieved March 24, 2019, from http://www.astronautix.com/i/is-a.html

[2] Garcia, M. (2017). Space Debris and Human Spacecraft. National Aeronautics and Space Administration. Retrieved March 24, 2019, from https://www.nasa.gov/mission_pages/station/news/orbital_debris.html

[3] Senechal, T. (2007). Orbital debris: Drafting, negotiating, implementing a convention. Massachusetts Institute of Technology. Retrieved March 24, 2019, from http://web.mit.edu/stgs/pdfs/Orbital%20Debris%20Convention%20Thierry%20Senechal%2011%20May%202007.pdf

[4] Stansbery, E. (n.d.). Orbital Debris Optical Measurements. National Aeronautics and Space Administration. Retrieved March 25, 2019, from https://orbitaldebris.jsc.nasa.gov/measurements/optical.html

[5] Klinkrad, H. (2004). Monitoring Space- Efforts Made by European Countries. European Space Agency. Retrieved March 25, 2019, from https://fas.org/spp/military/program/track/klinkrad.pdf

[6] Dunbar, B. (2008). STS-76 Mir Environmental Effects Payload (MEEP). National Aeronautics and Space Administration. Retrieved March 25, 2019, from https://orbitaldebris.jsc.nasa.gov/measurements/optical.html

[7] Brandt, E. (2017). Lidar vs Radar: Pros and Cons of Different Autonomous Driving Technologies. The Drive. Retrieved March 25, 2019, from https://www.thedrive.com/sheetmetal/16916/lidar-vs-radar-pros-and-cons-of-different-autonomous-driving-technologies

[8] (2019). Lidar vs. Cameras for Self Driving Cars – What's Best?. Autopilot Review. Retrieved March 25, 2019, from https://www.autopilotreview.com/lidar-vs-cameras-self-driving-cars/

[9] Gleghorn, G. (1995). Orbital Debris: A Technical Assessment. The National Academy Press. Retrieved February 27, 2019, from https://www.nap.edu/read/4765/chapter/7#80

[10] Englert, C. R., Bays, J. T., Marr, K. D., Brown, C. M., Nicholas, A. C., Finne, T. T. (2014). Optical orbital debris spotter. Acta Astronautica, 104(1), 99-105.

[11] "NOAA Climate Data Record (CDR) of Solar Spectral Irradiance (SSI)" https://data.nodc.noaa.gov/cgi-bin/iso?id=gov.noaa.ncdc:C00899

[12] Rokinon Catalog "Rokinon 7.5mm f/3.5 Specifications" https://www.rokinon.com/lenses/digital-photo-lenses/75mm-f35

[13] Northumbria Optical Coating Catalog "Selected filter-Northumbria Optical Coatings Limited" https://www.noc-ltd.com/catalogue/band-pass/sbp-10577-001175

[14] Coherent Laser's Diamond series "Lasers with similar properties to desired SWEEP laser" https://www.coherent.com/lasers/laser/co2-and-co-lasers/diamond-c-series

[15] Edmund Optics product page "Conic mirror Diagram" https://www.edmundoptics.com/f/cone-mirrors/11556/

[16] Edmund Optics product page "Gold's Reflectance-Gold mirrors" https://www.edmundoptics.com/f/Gold-Off-Axis-Parabolic-Mirrors/39489/

[17] Optical Orbital Debris Spotter. Acta Astronautica. Retrieved March 25, 2019, from https://www.sciencedirect.com/science/article/pii/S0094576514002872?via%3Dihub

[18] Pt. Grey Blackfly S High Resolution Video Camera. Pt. Grey. Retrieved March 25, 2019, from https://www.ptgrey.com/blackfly-s-50-mp-color-gige-vision-sony-imx264

[19] Magellan Power Control Unit. Retrieved April 9, 2019. http://magellan.aero/wp-content/uploads/PCU%20-%20Web%20Version.pdf

[20] Lithium-Ion Aerospace Battery, Eagle Picher. Retrieved April 9, 2019, from: https://www.eaglepicher.com/sites/default/files/EP%20SAR%2010211%20DATA%20SHEET.pdf

[21] AWG American Wire Gauge Diameter Chart. Retrieved April 9, 2019, from: https://daycounter.com/Calculators/AWG.phtml

[22] AWG Copper Wire Size Table and Data Chart @ 100 degrees F | Engineer's Edge. Retrieved April 9, 2019, from: https://www.engineersedge.com/copper_wire.htm

[23] Plante, J. Lee, B., Environmental Conditions for Space Flight Hardware: A Survey (2004). Internal NASA Parts and Packaging Program Report. Retrieved February 22, 2019 https://nepp.nasa.gov/docuploads/...0469.../environmental%20Testing%20Survey.doc

[24] Meseguer, J, et al. (2012). Spacecraft Thermal Control. Woodhead Publishing in Mechanical Engineering. Retrieved March 8, 2019, from https://books.google.com/books?id=_dpkAgAAQBAJ&lpg=PP1&hl=en&pg=PA22#v=onepage&q&f=false

[25] Menezes, R. (2017). How to Convert Wattage to Degrees. Leaf Group. Retrieved February 27, 2019, from https://sciencing.com/how-8643971-convert-wattage-degrees.html

[26] Hyers, R. (2013). Lightweight, High-Temperature Radiator for Space Propulsion. University of Massachusetts. Retrieved February 27, 2019, from https://ntrs.nasa.gov/archive/nasa/casi.ntrs.nasa.gov/20130001608.pdf

[27] Juhasz, A. J. (2002). Design Considerations for Lightweight Space Radiators Based on Fabrication and Test Experience With a Carbon-Carbon Composite Prototype Heat Pipe. Revised. https://ntrs.nasa.gov/archive/nasa/casi.ntrs.nasa.gov/19980236936.pdf

[28] Product Bulletin. Sheldahl. Retrieved March 8, 2019, from https://www.sheldahl.com/sites/default/files/2017-09/ITO%20-%20GE.pdf

[29] Ketsdever, A. (2014). Attitude Determination and Control. University of Colorado Springs. Retrieved February 11, 2019, from eas.uccs.edu/~aketsdev/...files/Attitude%20Determination%20and%20Control.ppt

[30] Reaction Wheels. (n.d.). Sinclair Interplanetary. Retrieved February 11, 2019, from http://www.sinclairinterplanetary.com/reactionwheels

[31] Reaction Wheels. (2019). Blue Canyon Tech. Retrieved March 11, 2019, from https://bluecanyontech.com/wp-content/uploads/2018/07/DataSheet_RW_09.pdf

[32] Larson, W., et al. (1979). Space Mission Analysis and Design 3rd Edition. United States Airforce Academy. Retrieved March 20, 2019, from https://the-eye.eu/public/WorldTracker.org/Space/Space%20Engineering/Space_Mission_Analysis_and_Design.pdf

[33] Star Tracker Selection Retrieved February 19th 2019 T1 https://www.terma.com/media/471442/t1_t2_star_tracker_rev2.pdf

[34] Inertial Measurement Unit (IMU) Selection LN-200S Retrieved February, 20th 2019 https://www.northropgrumman.com/Capabilities/LN200FOG/Documents/ln200s.pdf

[35] Sun Sensor Selection Retrieved February 20th 2019 http://bradford-space.com/products-aocs-fine-sun-sensors.php#

[36] MAG-3 Three Axis Magnetometer http://www.spacequest.com/s/MAG-3-Datasheet-Ver-20160621.pdf

[37] NEMO Non-Volatile Flash Based Scalable Recorder." Airbus Defense and Space Equipment spaceequipment.airbusdefenceandspace.com/payload-products/payload-data-handling-with-memory/nemo/

[38] Jetson Nano Board for Image Processing https://developer.nvidia.com/embedded/buy/jetson-nano-devkit

[39] Vu, Nancy, "The FireSat Project" (2010). Systems Engineering Research Projects and Oral Presentations. 32. http://digitalcommons.lmu.edu/se_etdrps/32

[40] Orbital Debris Program Office https://orbitaldebris.jsc.nasa.gov/

[41] Peet, M. M. (2018). Converting to/from r and v. Lecture presented at Spacecraft Dynamics and Control in Arizona State University.

[42] Wertz, J. R., Wertz, J. R., Everett, D. F., and Puschell, J. J., Space mission engineering the new SMAD, Hawthorne, CA: Microcosm, 2015.

[43] Vallado, D. A., and McCain, W. D., Fundamentals of Astrodynamics and Applications.

[44] Siahpush, Ali., Gleave, Janet,. A Brief Survey of Attitude Control Systems for Small Satellites Using Momentum Concepts. Honeywell Inc. Satellite Systems Division Glendale. Arizona https://pdfs.semanticscholar.org/3c34/14d7d2a379ec103107877e8399b83b4e67dc.pdf

[45] Janson, Siegfried W,. Brane Craft, The Aerospace Corporation Space Sciences and Application Laboratory, El Segundo, CA (Feburary 1st 2017). https://www.nasa.gov/sites/default/files/atoms/files/niac$_2$016$_p$hase$i_j$anson$_b$raneconcept$_t$agged.pdf